biomedicines

MDPI

Concept Paper

A Mathematical Model for Determining the Body's Fluctuating Need for and Synthesis of Active Vitamin D

Sean R. Maloney

Department of Rehabilitation Medicine, W.G. (Bill) Hefner VA Medical Center, 1601 Brenner Avenue, Salisbury, NC 28144, USA; sean.maloney@va.gov; Tel.: +1-336-406-6626 or +1-704-638-3468; Fax: +1-704-638-3811

Abstract: The process by which $1,25(OH)_2D_3$ is synthesized and degraded and how it is transported out of the cell and body is described. The changing demand for the synthesis of $1\text{-}25(OH)_2D_3$ during different conditions experienced by the body is reviewed. A method of determining $1,25(OH)_2D_3$ synthesis and demand, and the percent utilization of $25(OH)D_3$ to make $1,25(OH)_2D_3$ is presented based on the measurement of the end metabolites of $1,25(OH)_2D_3$ and of its immediate precursor, $25(OH)D_3$. A mathematical model has been developed to allow the calculation of $1,25(OH)_2$ D synthesis, and demand, and the percent utilization of $25(OH)D_3$. Simple algebraic equations have been derived which allow the calculation of these new parameters using the concentrations of the end metabolites of $1,25(OH)_2D_3$ and its immediate precursor, $25(OH)D_3$ in the serum and urine. Vitamin D plays an important role in combating invading bacteria and viruses and in subduing the body's associated inflammatory response. This new approach to evaluating vitamin D status may help clinicians determine $25(OH)D_3$ and $1,25(OH)_2D_3$ levels needed to suppress bacterial infections, viral replication during new viral infections and the reactivation of latent viruses, and to downregulate the inflammatory responses caused by bacteria and viruses.

Keywords: 25-hydroxyvitamin D; 1,25-dihydroxyvitamin D; immune system receptors; inflammatory response; COVID-19

Citation: Maloney, S.R. A Mathematical Model for Determining the Body's Fluctuating Need for and Synthesis of Active Vitamin D. *Biomedicines* **2023**, *11*, 324. https://doi.org/10.3390/biomedicines11020324

Academic Editor: Yan-Ru Lou

Received: 20 November 2022
Revised: 3 January 2023
Accepted: 9 January 2023
Published: 24 January 2023

1. Introduction

Vitamin D is a fat-soluble vitamin and a hormone that has receptors in many tissues of the body. It plays an important role in many different normal and abnormal conditions that routinely affect the human body. One of the first roles that was discovered for vitamin D was the maintenance of normal calcium and phosphorous levels in bone in order to prevent rickets in children and osteoporosis in adults. It is necessary for maintaining normal muscle strength. It has a very important role in immune system function in order to fight off infection and modulate the inflammatory response to infection. It is important for a developing embryo and fetus during pregnancy. Finally, there is growing evidence that it is important to reduce the risk of heart disease, type 2 diabetes, cancer, and the risk of premature death and cognitive decline [1].

There have been numerus studies recently which have linked increased COVID-19 morbidity and mortality to low vitamin D states [2–6]. Likewise, there have been recent review articles which discuss reasons why low vitamin D states may play a role in a patient's ability to fight off or mitigate the morbidity and mortality associated with a COVID-19 infection [7–9]. Central to this new focus on vitamin D status is the important role that vitamin D plays in the modulation of the immune system [10–12]. Immune system cells with vitamin D receptors exist in large numbers in many tissues of the body including primary lymphoid organs (bone marrow and thymus) and secondary lymphoid organs (lymph nodes, the spleen, the tonsils, skin, and various mucous membrane layers in the body including those of the nose, throat, and bowel) [13]. An important recent article reviews the relationship between co-morbidities in COVID-19 patients known to be

associated with increased morbidity and mortality and those same co-morbidities in low vitamin D states [14].

Persistent low vitamin D states may chronically impair the immune system in individuals in two ways. First, in low vitamin D states, the immune system may be unable to maximally suppress viruses such as COVID-19 in part due to inadequate production of cathelicidin and defensin β2 [15–17]. Second, vitamin D is a hormone which acts directly on the immune system including B and T lymphocyte cells to downregulate the inflammatory reaction triggered by viral antigens, or other microorganisms [18].

Plasma 25(OH)D_3 vitamin D precursor levels represent vitamin D stores in the body and have been traditionally measured to assess vitamin D status. This paper will build on and review evidence supporting the following two premises: (1) plasma 25(OH)D_3 levels do not consistently represent 1,25$(OH)_2D_3$ synthesis (or total body levels), demand for 1,25$(OH)_2D_3$, or percent utilization of 25(OH)D_3 to form 1,25$(OH)_2D_3$ by the body, and (2) the need for and utilization of active vitamin D by tissues of the body can vary between individuals and dramatically in the same individual under different circumstances. Many factors can reduce a person's ability to produce active vitamin D including low vitamin D precursor stores, increased body mass index, BMI (i.e., obesity) which dilutes the concentration of vitamin D precursor in the serum, decreased exposure to ultra-violate B, UVB, light, increasing age, exogenous medications, and genetic factors.

The measurement of active vitamin D, 1,25$(OH)_2D_3$, plasma levels is possible and in certain situations is indicated. This paper will present information to support the premise that serum active vitamin D levels often do not correlate with vitamin D precursor levels and may not correlate well with active vitamin D synthesis in the body.

2. Methods

2.1. Vitamin D Molar Balance Model

A molar balance approach to analyze active vitamin D synthesis and degradation is presented in this paper. Instead of focusing on the front end (input) of the vitamin D synthesis pathway, this paper will focus only on the final metabolism of active vitamin D and its immediate precursor. This molar balance approach may permit (1) an estimation, at one point in time (t), of the amount of active vitamin D that has been recently produced in the body, (2) the determination (based on measurable quantities) of the synthesis of active vitamin D, 1,25$(OH)_2D_3$, over 24 h, and (3) the evaluation of the body's overall demand for 1,25$(OH)_2D_3$ at a given point in time (t). Overall demand will be determined by comparing the amount of active vitamin D precursor, 25(OH)D_3, used to synthesize active vitamin D to the amount of active vitamin D precursor, that is diverted away from the synthesis of active vitamin D and metabolized (wasted). Knowing the demand for 1,25$(OH)_2D_3$, and the percent utilization of active vitamin D precursor to produce active vitamin D, may help to determine whether inadequate, adequate, or excess vitamin D precursor is present. Measurement of the above vitamin D characteristics may enable clinicians to better identify individuals who may have impaired immune system function associated with inadequate active vitamin D synthesis and to better treat these individuals when they have COVID-19 viral or other acute infection infections. Similarly, measurement of these characteristics may allow clinicians to better treat those individuals with chronic inflammation associated with partially reactivated, latent viruses.

The 25(OH)D_3 molar balance model is depicted qualitatively in Figure 1. This figure provides a diagrammatic picture of the movement of vitamin D through the body and between the intracellular and extracellular compartments of the body. The blue arrow in Figure 1 depicts an intracellular synthesis pathway for 1,25$(OH)_2D_3$ without its immediate precursor, 25(OH)D_3, ever having to pass through or to be initially stored in the extracellular plasma space.

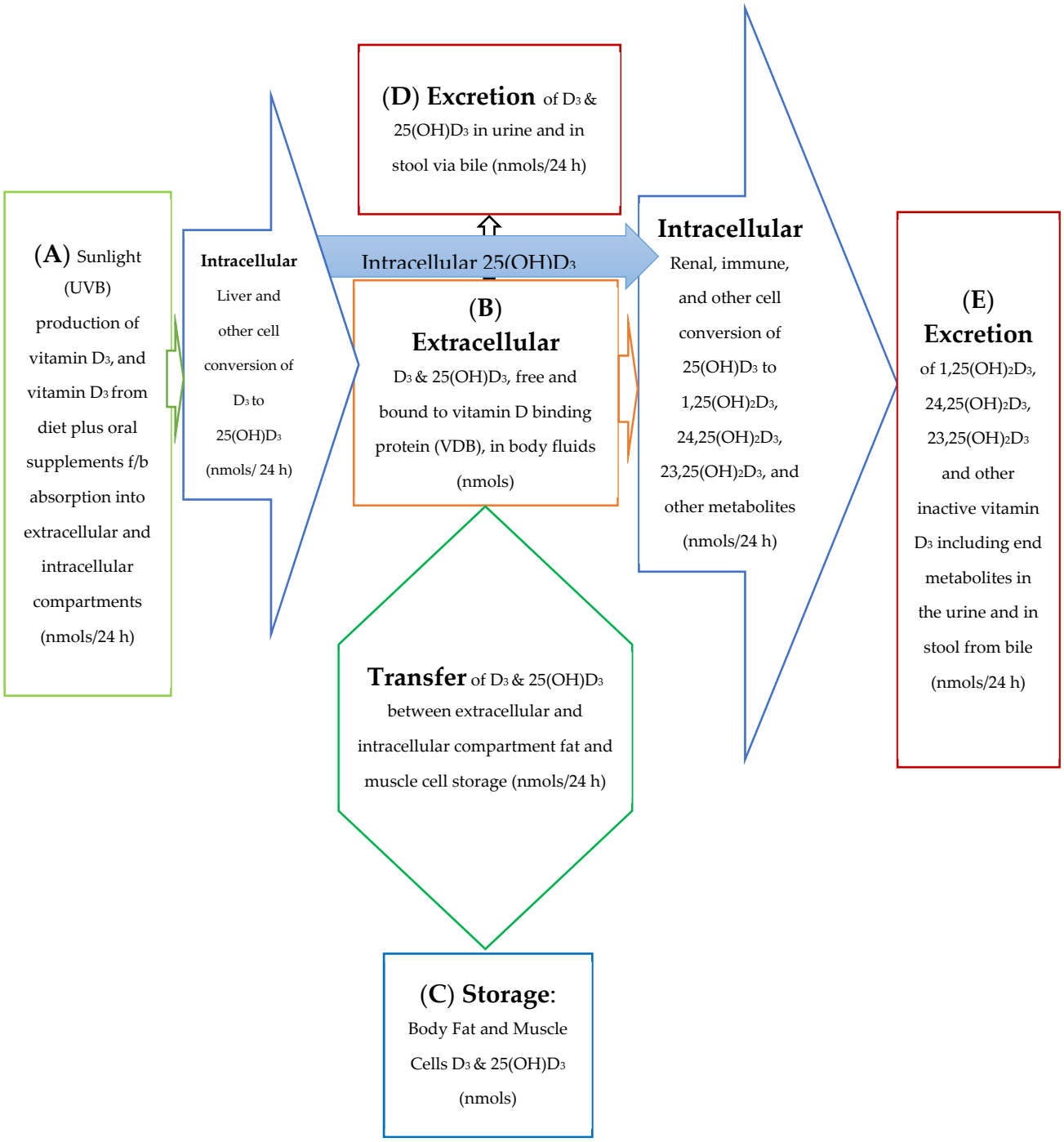

Figure 1. Model for Absorption, Synthesis, Transport, Conversion, Storage, and Excretion of vitamin D Precursors and Metabolites by the Body.

The molar balance model is described quantitatively in several equations included in this text as well as in a more rigorous manner in the Appendix A. The figures and equations included in this text along with the Appendix A describe the active vitamin D precursor ($25(OH)D_3$) transport, conversion to active vitamin D, metabolism, and excretion from the body. In this molar balance model, the body is divided into two main compartments for simplicity. The extracellular compartment is made up of all those spaces in the body which are not made up of cells and which contain fluids such as plasma, lymphatic fluid, bile, interstitial fluid, etc. The intracellular compartment is the space made up all those cells in

the tissues of the body. It is important to remember that the synthesis of active vitamin D and its breakdown to its end metabolites is an intracellular process. See Figure 2a,b below.

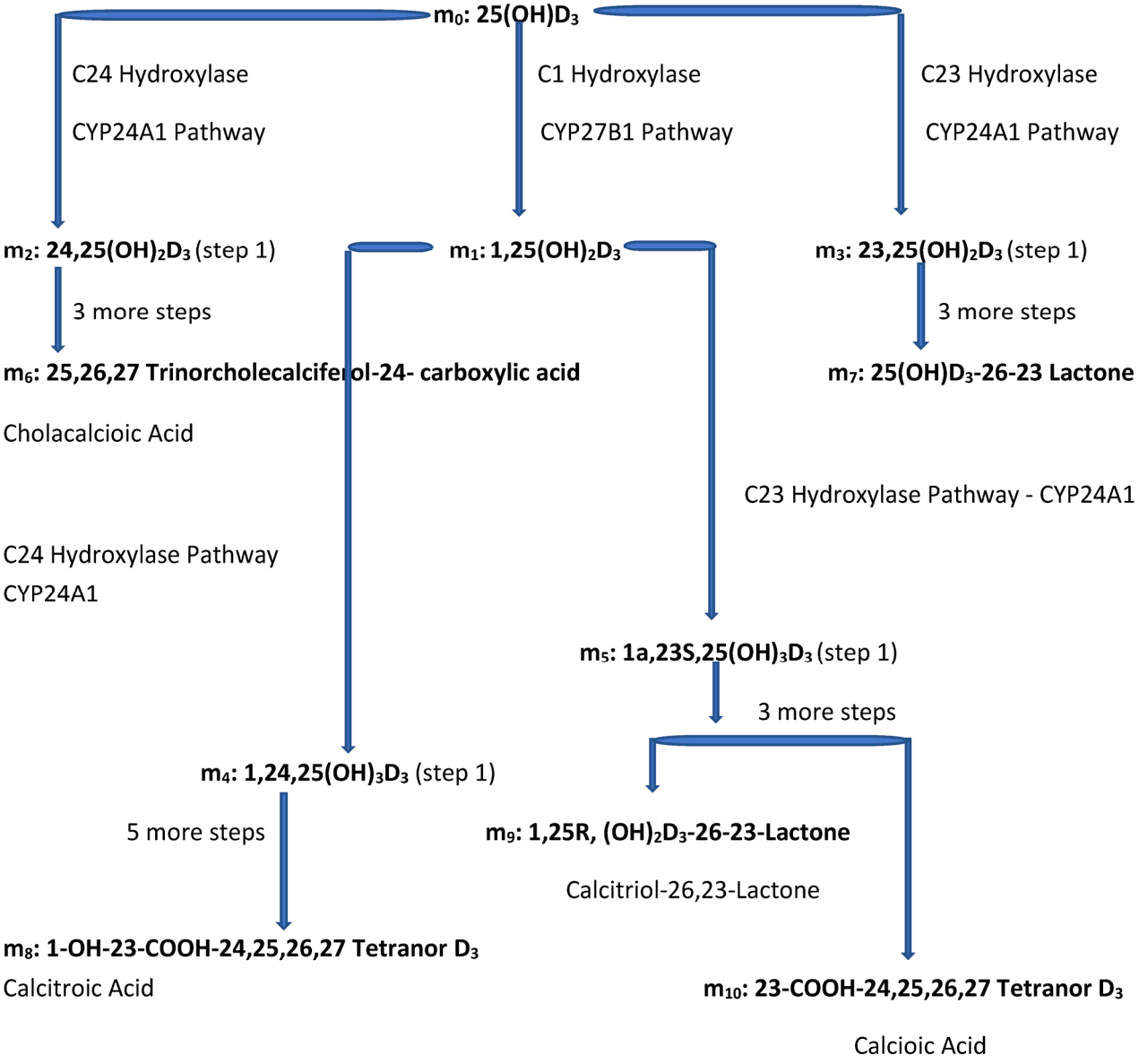

(**a**)

Figure 2. *Cont.*

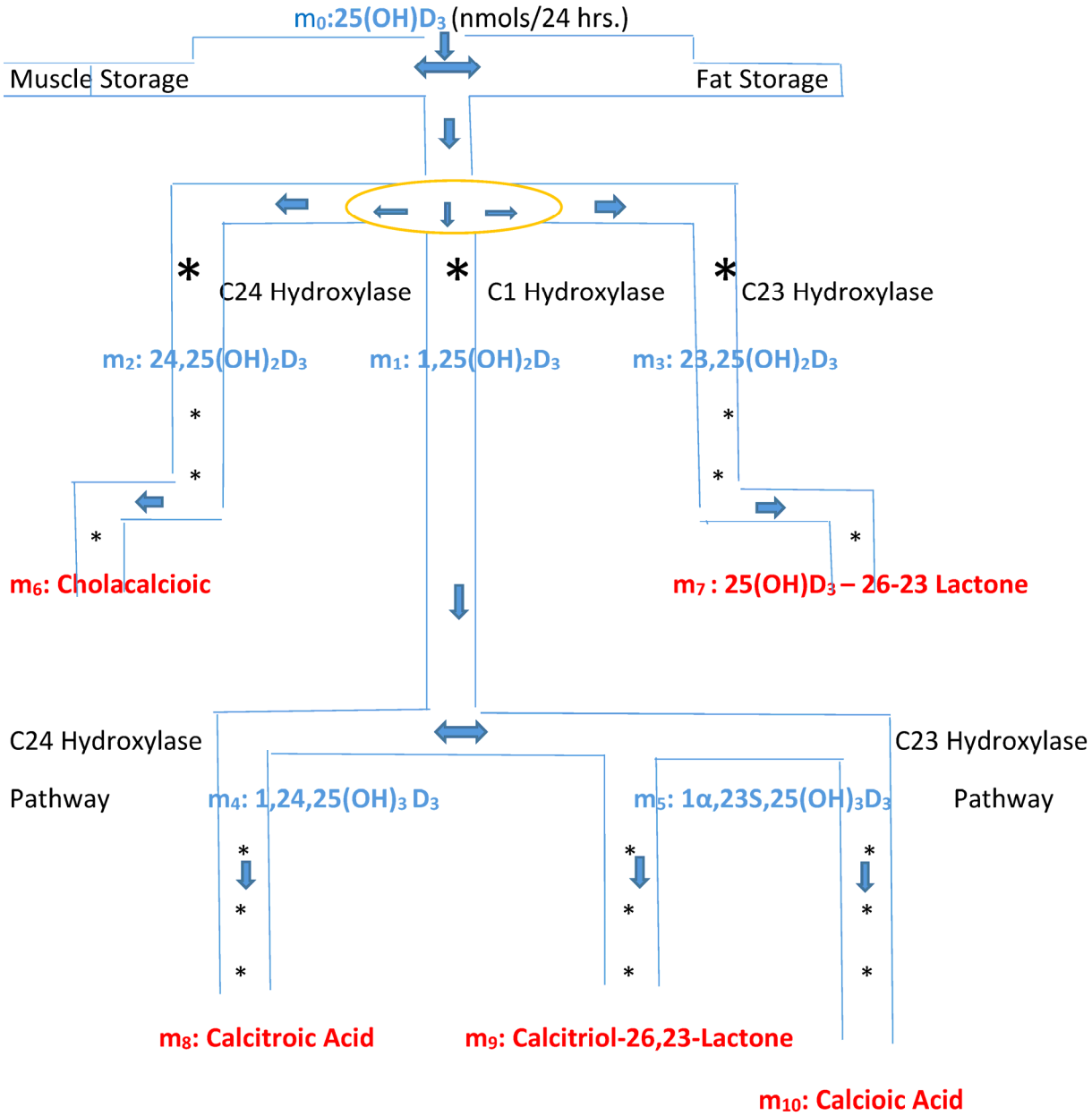

(**b**)

Figure 2. *Cont.*

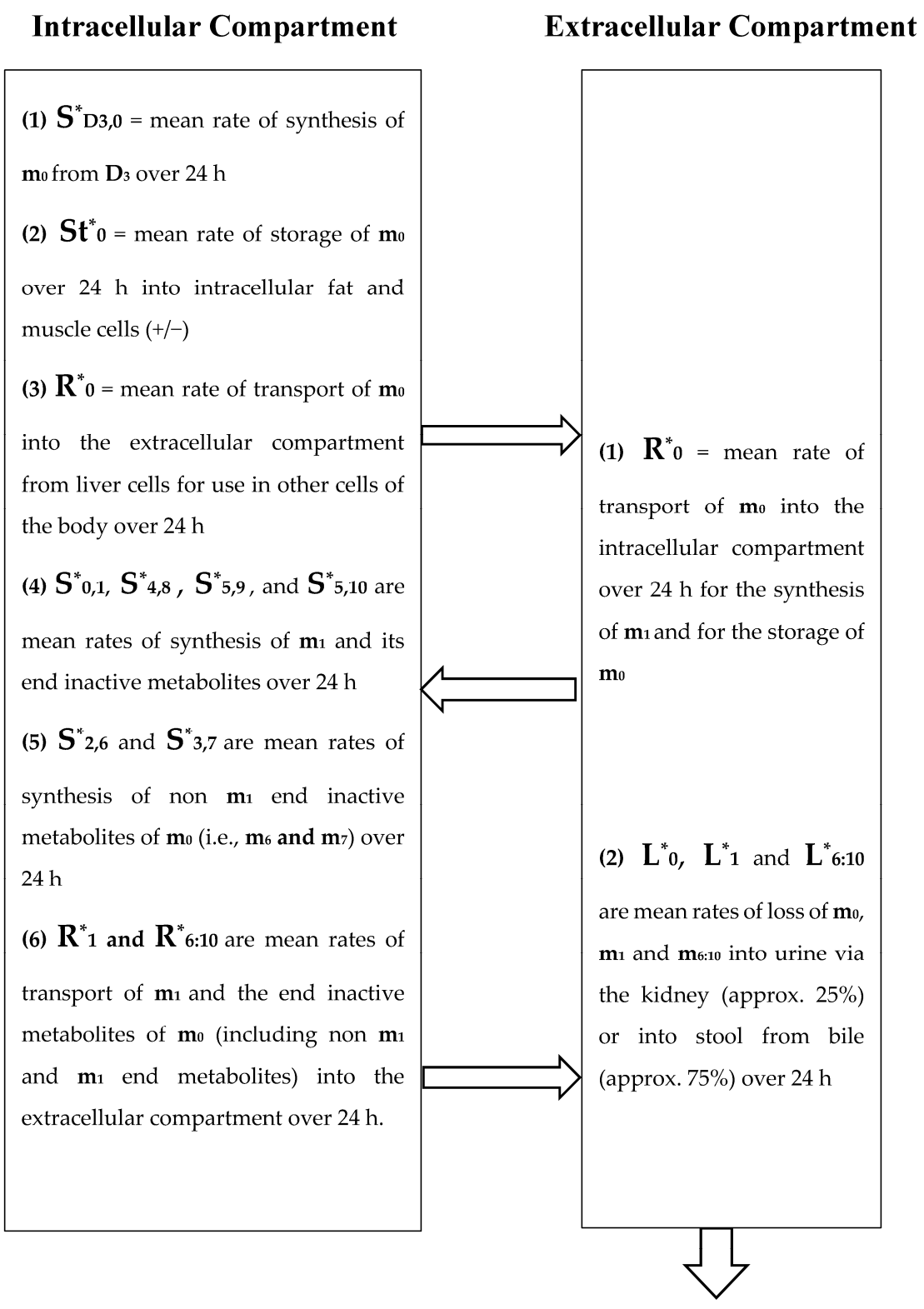

(**c**)

Figure 2. *Cont.*

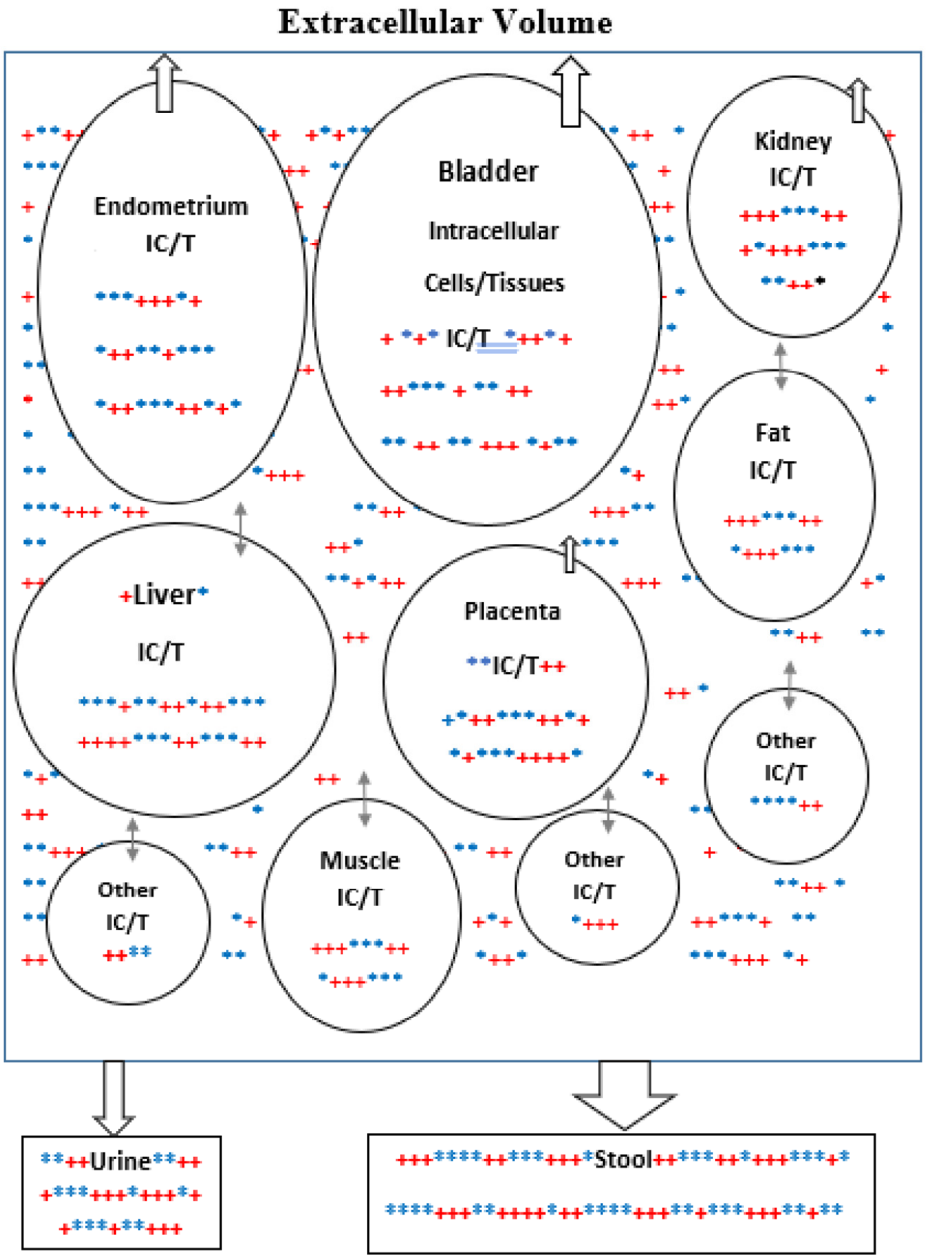

(**d**)

Figure 2. (**a**) Intracellular Vitamin D Pathways Describing the Conversion of 25(OH)D_3, m_0, to Its Initial and End Metabolites, m_n. The C in front of the enzymes represents the carbon atom location which is acted upon by the pathway enzyme. The m_n terms describe the initial, some of the intermediate, and the end metabolites of m_0. The end metabolites (m_6 to m_{10}) pass from the intracellular to the extracellular compartments and are excreted in urine (approx. 25%) and in stool (approx. 75%). (**b**) Depicted in this Flow Diagram is the Intracellular Metabolism of 25(OH)D_3, m_0, to Its Initial Metabolites (m_1, m_2, and m_3), and to its End Metabolites in red (m_6 and m_7) that are diverted away from active vitamin synthesis. Also depicted is the Intracellular Metabolism of 1,25$(OH)_2$, m_1 and its End Metabolites in red (m_8, m_9, and m_{10}). In this flow diagram, the m_n terms represents the initial and end metabolites of m_0 (i.e., m_1 through m_{10}). The large bold * symbols represent the enzymes for the synthesis of the initial metabolites of m_0 (25(OH)D_3). The small groups of three * symbols represent the enzymes which regulate the amount of end metabolites of active vitamin D hormone, m_1, and the enzymes which regulate the amount of end metabolites of m_0 diverted away from m_1 synthesis in response to a changing need by the body for active vitamin D.

(**c**) Model of the Body's Synthesis, Transport, and Excretion of m_0 [25(OH)D_3], m_1 [1,25(OH)$_2D_3$] and their End Metabolites, m_6 to m_{10} (nmols/24 h). (**d**) Simple Model of the Body's Composition of Non m_1 End Metabolites from [25(OH)D_3], m_6 and m_7 (*), and End Metabolites from m_1 [1,25(OH)$_2D_3$], m_8 to m_{10} (+), at any point in time, t, in moles. The open space in the box is the extracellular space and the circles/ovals represent the intracellular space/tissues (IC/T). The size of the arrows indicates the amount of CYP24A1 enzyme RNA in the IC/T and the potential for CYP24A1 synthesis and ultimately the ability for metabolism of 25(OH)D_3 and 1,25(OH)$_2D_3$ to their end metabolites.

For the purpose of this model, the spaces which are made up of urine in the bladder and stool in the distal small bowel and large bowel are considered outside the body and the end metabolites of vitamin D are assumed lost to the intracellular and extracellular spaces of the body once they enter urine and stool in these spaces. The cells of bladder and bowel tissues including the cells of their mucosal linings are in the intracellular space/compartment of the body (see Figure 2c).

This model describes the synthesis and transport of active vitamin D, 1,25(OH)$_2D_3$, and its inactive metabolites into and out of the intracellular and extracellular compartments of the body at any arbitrary time (t) and over an arbitrary, 24 h, interval of time. The relationship between the end inactive metabolites of 1,25(OH)$_2D_3$ and the end inactive metabolites of 25(OH)D_3 (that are diverted away from 1,25(OH)$_2D_3$ synthesis, i.e., wasted) are used to establish changing 1,25(OH)$_2D_3$ demand and changing vitamin D precursor, 25(OH)D_3, utilization by the body to synthesize active vitamin D.

This model may also provide a better understanding of why: (1) the same store or concentration of 25(OH)D_3 in the plasma may result in different overall (increased or decreased) rates of 1,25(OH)$_2D_3$ synthesis in cells of the tissues of the body, (2) the same store or concentration of 25(OH)D_3 in the plasma may result in an inadequate rate of 1,25(OH)$_2D_3$ synthesis for one individual but not for another or for one individual experiencing increased 1,25(OH)$_2D_3$ demand over their usual vitamin D demand state [19–21]. and (3) a significant portion of D_3 can be converted from vitamin D_3 to 25(OH)D_3 and then to 1,25(OH)$_2D_3$ in the same cell without this portion of the body's vitamin D precursor, 25(OH)D_3, ever passing through the plasma (sub-extracellular) space before being converted to 1,25(OH)$_2D_3$ [22]. The active form of vitamin D is a hormone and is structurally different from its precursor molecules and its inactive metabolites. This difference allows active vitamin D to attach to receptor sites in or on target cells in order to activate different genes and chemical reactions. As a result of a body's changing demand or need for active vitamin D, cells/tissues in the body can produce increasing or decreasing amounts of the active form of vitamin D, 1,25(OH)$_2D_3$, from its precursor, 25(OH)D_3. The source of vitamin D precursor needed for this synthesis can come from vitamin D precursor already present in the body's cells/tissues, or from vitamin D precursor entering the body's cells/tissues from the plasma space.

The changing need for active vitamin D can occur in cells/tissues which cannot completely synthesize their own active form of vitamin D but rely on plasma vitamin D precursor, 25(OH)D_3, or rely on active vitamin D, 1,25(OH)$_2D_3$ from other cells/tissues of the body (endocrine source). There are also the cells/tissues that can synthesize their own active vitamin D (autocrine or paracrine source for active vitamin D). Thus, some cells/tissues that store vitamin D precursors, can produce their own active vitamin D independently of the extracellular plasma source of the vitamin D precursor, 25(OH)D_3.

Changing demand and synthesis of active vitamin D has been documented in several studies. One recent study which compared active vitamin D serum levels in non-pregnant women with those in pregnant women found significantly increased active vitamin D levels in those who were pregnant. Mean levels of active vitamin D, 1,25(OH)$_2D_3$, at 15 weeks were as follows: non-pregnant controls, 85.6 picomoles per liter (pmols/L), non-preeclamptic pregnant women, 336.3 pmols/L, and preeclamptic pregnant women 388.8 pmols/L [23]. Mean serum 25(OH)D_3 levels in the same groups, respectively, were 46.8 nmols/L, 44.7 nmols/L, and 33.1 nmols/L. In the first two groups of women, mean

serum 25(OH)D_3 levels were similar, but mean serum 1.25(OH)$_2D_3$ levels varied by a factor of 4.

In comparing the mean serum 25(OH)D_3 levels of the last two groups of pregnant women, the pre-eclamptic women had a lower mean serum 25(OH)D_3 level but a higher mean serum 1,25(OH)$_2D_3$ level. These findings represent a dramatic example of uncoupling of mean serum 25(OH)D_3 and 1,25(OH)$_2D_3$ levels when comparing non-pregnant and pregnant women's levels and to a lesser extent when comparing pregnant and pre-eclamptic pregnant women's levels.

An increase in vitamin D utilization/demand has been documented by serial measurements of dropping serum vitamin D precursor, 25(OH)D_3 levels during military training of short duration [24]. During a 1993 study of nutritional status in young healthy US Army soldiers undergoing an arduous 21-day Special Forces Evaluation and Selection Program, serum vitamin D precursor, 25(OH)D_3 levels dropped from an initial mean level of 61 ng/mL (range 34–100 ng/mL) on the first day to a mean level of 55 ng/mL (range 38–97 ng/mL) on day 10, to a mean level of 51 ng/mL (range 42–60) by day 20. The statistical significance of this drop was not tested at the time perhaps in part because vitamin D was only one of many nutritional status biomarkers that were measured and because mean vitamin D levels remained above the upper limits of normal (50 ng/mL at the time). To approximately convert ng/mL to nmols/L, multiply ng/mL by 2.5.

Vitamin D binding protein and total and free vitamin D metabolites have been shown to have a changing or diurnal rhythm (i.e., repeated daily pattern of change in vitamin D metabolite levels during the day) [25]. A recent case study of a middle-aged woman, who was taking 5000 IUs of vitamin D_3 orally each afternoon for over one year, demonstrated not only a daily serum 25(OH)D_3 diurnal rhythm but also a temporary significant drop in serum 25(OH)D_3 level associated with an acute but short duration respiratory illness [26]. The study included four separate days of evaluation, 11 October, 18 October, 15 November, and 28 November 2017) and the midday serum 24(OH)D_3 levels on each of these days was: 67 ng/mL, 65 ng/mL, 51 ng/mL (at the time of a brief cold), and 67 ng/mL, respectively. The approximate drop of 25% on day three was significant, $p < 0.013$.

The level of vitamin D precursor, 25(OH)D_3, in the plasma is often not proportional to the level of active vitamin D, 1,25(OH)2D_3 in the plasma and does not directly indicate the rate of active vitamin D synthesis in all the tissues of the body. This occurs in part because paracrine/autocrine 1,25(OH)$_2D_3$ can be synthesized and metabolized in cells/tissues of the body without active vitamin D precursor, 25(OH)D_3, passing from the plasma into the affected cell and without paracrine/autocrine produced active 1,25(OH)$_2D_3$ passing from the tissue/cells where it is produced and consumed into the plasma space. This observation is supported by the concurrent presence of the enzymes that allow the conversion of D_3 to 25(OH)D_3 and the enzyme that allows the conversion of precursor, 25(OH)D_3, to active vitamin D, 1,25(OH)2D_3, in some cells/tissues of the body. The enzymes (CYP2R1, CYP3A4, and CYP27A1) which convert D_3 to 25(OH)D_3, the enzyme (CYP27B1) which converts 25(OH)D_3 to 1,25(OH)$_2D_3$, and the enzyme (CYP24A1) which converts 25(OH)D_3 and 1,25(OH)$_2D_3$ to inactive forms of vitamin D (i.e., 24,25(OH)$_2D_3$, 23,25(OH)$_2$, 1,24,25(OH)$_3D_3$ and 1,23,25(OH)$_3D_3$) are described in more detail in other publications [27,28].

The RNA expression of these enzymes has been examined recently in 27 different tissues of 95 human subjects as part of a larger study of gene expression [29]. The units of gene transcript expression are RPKM (i.e., Reads per Kilobase of transcript, per Million mapped reads) [30]. In comparing/interpreting the RPKM reads, (i.e., comparing the ability of cells/tissues to produce 25(OH)D_3 and its metabolites), it is important to note that RPKM reads represent the density of RNA in the tissue sample and not the overall size of the tissue or organ. Thus, the ability of tissues and organs to produce enzymes or process substrate will also depend on the total relative size of the tissue or organ and other factors such as the rate of diffusion or perfusion of the substrates through the tissue. The following four paragraphs outline the presence of the enzymes of vitamin D metabolism in many of the cells/tissues of the body.

The CYP27A1 enzyme had the greatest representation in the body among the three enzymes which convert D_3 to 25(OH)D_3 [31]. Of the 27 tissues studied, liver was the tissue with the highest expression of this gene (approx. 101.4 RPKM), followed by small intestine (27.6 RPKM), lung (approx. 26 RPKM), and duodenum (approx. 23 RPKM). However, most of the other tissues examined had significant expression of this enzyme RNA including prostate (18 RPKM), kidney (18 RPKM), adrenal (12 RPKM), ovary (11 RPKM), brain-colon-urinary bladder (9 RPKM), lymph node tissue (8 RPKM) and fat (6 RPKM). The second most widely distributed enzyme RNA (but of lower concentration) for this first conversion, D_3 to 25(OH)D_3, was CYP2R1 [32]. This enzyme was most highly expressed in skin (2.2 RPKM). Other tissue representation included testes (2.0 RPKM), duodenum (approx. 1.27 RPKM), small intestine (1.25 RPKM), appendix (1.36 RPKM), lymph node tissue (1.1 RPKM), spleen (1.0 RPKM), fat and thyroid (0.9 RPKM) and bone marrow (0.45 RPKM). The third enzyme for the conversion of D_3 to the vitamin D_3 precursor, 25(OH)D_3 was CYP3A4 [33]. This enzyme was largely expressed in only three tissues: liver (476.5 RPKM), small intestine (282.8 RPKM), and duodenum (approx. 250 RPKM).

Enzyme CYP27B1 converts 25(OH)D_3 to the active form of vitamin D, 1,25$(OH)_2D_3$ [34]. Its RNA was present in almost all the tissues studied but most significantly present in kidney (9.5 RPKM) and thyroid (4.8 RPKM), followed by appendix (approx. 0.9 RPKM), lymph node (0.8 RPKM), bone marrow and adrenal tissue (0.4 RPKM), and fat (0.1 RPKM).

CYP24A1 is the enzyme which metabolizes both 25(OH)D_3 and 1,25$(OH)_2D_3$ to the inactive forms 24,25$(OH)_2D_3$, 23,25$(OH)_2D_3$, 1,24,25$(OH)_3D_3$, and 1,23,25$(OH)_3$, respectively, as well as to their end metabolites [28–35]. The catabolic CYP24A1 enzyme RNA is present in many tissues, and is highly present in urinary bladder (approx. 21.5 RPKM), and endometrium (10.7 RKPM), followed by kidney (approx. 3.5 RPKM), and placenta (approx. 2.5 RPKM). The high levels of CYP24A1 RNA and potential for this enzyme's synthesis in the endometrium and placenta may be required due to the increased 1,25$(OH)_2D_3$ synthesis during pregnancy (see Figure 2d).

The RNA expression study from which the above data are taken did not include skeletal muscle tissue, and it is not known if enzyme RNA, for both steps in the conversion of D_3 to 1,25$(OH)_2$ D_3, exists in skeletal muscle. However, CYP27B1 has been found to be present in skeletal muscle [36–38]. In this molar balance analysis, D2 and its metabolites, and C-3-epi-25(OH)D_3 and 1,25$(OH)_2$-3-Epi-D_3 are ignored to simplify the model [39].

The concurrent existence of DNA genes and their resulting RNA that code for enzymes capable of converting D_3 to 25(OH)D_3 (3 possible enzymes) and 25(OH)D_3 to 1,25$(OH)_2D_3$ (1 enzyme) in many different tissue locations suggests the existence of a synthesis pathway from D_3 to 1,25$(OH)_2D_3$ in cell/tissue types that are independent of the need for transported extracellular (plasma) compartment 25(OH)D_3 generated from the liver. The presence of RNA for a particular enzyme does not necessarily equate to a functional protein being translated from the RNA and the functionality of the proteins would need to be verified. The large presence of immune system cells in many tissues of the body makes the immune system potentially one of the largest producers and consumers of active vitamin D during certain conditions such as severe infections especially involving multiple tissues such as with COVID-19 virus infections.

An alternate, strictly intracellular, 1,25$(OH)_2D_3$ synthesis and degradation pathway supports the idea that extracellular (plasma) compartment 25(OH)D_3 and 1,25$(OH)_2D_3$ levels are partially uncoupled from intracellular compartment active vitamin D synthesis. An intracellular active vitamin D synthesis pathway independent of plasma, 25(OH)D_3, may explain why the rate of active vitamin D, 1,25$(OH)_2D_3$, synthesis is partially independent from the aqueous (plasma) vitamin D precursor, 25(OH)D_3 concentration.

Serum 25(OH)D_3 levels and 1,25$(OH)_2D_3$ levels do not appear to have a proportional relationship, and serum 25(OH)D_3 concentration in the plasma space may not necessarily reflect the body's ability to meet the need for active vitamin D synthesis. The following mathematical equations for the molar balance analysis are based on and depend on the accurate measurement of changing concentrations of vitamin D end metabolites in plasma

and urine samples. This model can be used to estimate active vitamin D synthesis and to assess whether the body's demand for vitamin D is being met. This molar balance method, of assessing vitamin D status, analyzes and depends on primarily the backend of the vitamin D metabolic pathway rather than the frontend.

Some data concerning where vitamin D_3 and 25(OH)D_3 are stored in the body exist based on intravenous radiolabeled vitamin D studies. D_3 has been shown to accumulate the most in adipose tissue but D_3 also accumulates in muscle, skin, plasma, and other organs. Total body storage of vitamin precursors has been estimated to be approximately 1 micro-mole (10^{-6} moles) with two-thirds stored as D_3 (primarily in adipose tissue) and the rest primarily stored as 25(OH)D_3 in various tissues and fluids including adipose tissue 35%, muscle 20%, and plasma/extracellular fluid 30% [40,41]. The molar balance model divides the storage of vitamin D into two compartments: intracellular and extracellular. Plasma is considered a sub-space of the extracellular compartment. The concentrations of 25(OH)D_3, 1,25$(OH)_2D_3$ and their end metabolites are assumed to be approximately uniform or homogeneous in both the plasma and total extracellular spaces. In contrast, levels of vitamin D precursors and active vitamin D are not assumed to be homogeneous within the cells/tissues of the intracellular compartment or spaces.

Using radioactive H^3 tagging, attempts have been made in several studies to determine the portion of vitamin D and its metabolites excreted in the urine verses in the stool (through bile) [42–44]. In three studies approximate differences between excretion in the urine verses in the stool have been as follows: 32% versus 68% (n = 7), 25% versus 75% (n = 7), and 22% versus 78% (n = 16). The molar balance model uses the values of 25% excretion in the urine and 75% in the stool.

2.2. Model Assumptions

1. Constant Compartment Volumes

The volume of the body's extracellular compartment or space, V_e, (or plasma sub-compartment, V_p) can change in certain circumstances such as pregnancy, severe dehydration, or congestive heart failure. However, for our model, it is assumed that the extracellular (or plasma) volumes at some initial time, t_0, $V_e(t_0)$, equals the extracellular compartment volume at some later time, t_1, $V_e(t_1)$, and equals a constant V_e. Similarly, the body's intracellular volume, V_i is assumed to be constant [45,46]

2. Intracellular volume = 2 × Extracellular Volume

For a complete list of different volume assumptions for men and women, see Table 1, "Intracellular and Extracellular Compartment Volume Analysis", and Table 2, "Total Male and Female Intracellular, Extracellular, and Plasma Volumes".

Table 1. Intracellular and Extracellular Compartment Volume Analysis.

Water Makes up Approximately 60% of Body Weight in the Male and 55% Body Weight in the Female	
For a 55 kg female:	
1.	Extracellular Compartment Volume ($\mathbf{V_e}$) = 's about 11 L [including plasma volume ($\mathbf{V_{pla}}$) 2.5 L, + Interstitial volume ($\mathbf{V_{inter}}$) 8.5 L + transcellular volume ($\mathbf{V_{trans}}$) 0.4 L–aver.]
2.	Intracellular Compartment Volume ($\mathbf{V_i}$) ='s about 22 L
3.	$\mathbf{V_i}$ = 's about $2\mathbf{V_e}$ and in females $\mathbf{V_e}$ equals about $4.4V_{pla}$ Ref. [45]
4.	Approx. mean HCT 40% (range 36–44%) my.clevelandclinic.org/health/diagnostic17683-hematocrit/results-and-follow-up, assessed on 8 March 2020
For a 70 kg Male:	
5.	Extracellular Compartment Volume ($\mathbf{V_e}$) = 's about 14 L [including plasma volume ($\mathbf{V_{pla}}$) 3.0 L, + Interstitial volume ($\mathbf{V_{inter}}$) 10.5 L + transcellular volume ($\mathbf{V_{trans}}$) 0.5 L–aver.]
6.	Intracellular Compartment Volume ($\mathbf{V_i}$) = 's about 28 L

Table 1. *Cont.*

	Water Makes up Approximately 60% of Body Weight in the Male and 55% Body Weight in the Female
7.	$\mathbf{V_i}$ = 's about $2\mathbf{V_e}$ and in males V_e equals about $4.66V_{pla}$ Ref. [46]
8.	Approx. mean hematocrit, HCT, 45.5% (range 41–50%) my.clevelandclinic.org/health/diagnostic17683-hematocrit/results-and-follow-up assessed on 8 March 2020

Differences between average male and female volumes are as follows: Plasma volume—males have 20% greater volume based on average size; Extracellular volume—males have 27% greater volume based on average size; Intracellular volume—males have 27% greater volume based on average size; Because of the differences in mean % hematocrit as well as physical size between men and women, the total % difference in aqueous volume (extracellular + intracellular) between men and women would be a difference of 42 L/33 L × 100% or 127%.

Table 2. Total Male and Female Intracellular, Extracellular, and Plasma Volumes.

For Males V^{e+i} = 42 L	**For Females V^{e+i} = 33**
V_i = 28 L	V_i = 22 L
V_e = 14 L	V_e = 11 L
V_p = 3 L	V_p = 2.5 L

3. The C_n Intracellular Concentration of End Metabolites = β Times the C_n Extracellular Concentration

The mean intracellular concentrations of the end metabolites, m_n, will be assumed to be proportional to and a factor β times the same concentrations in the extracellular compartment. The β factor is greater than 1 in this model because the end metabolites are assumed to be transported from the intracellular compartment (where they are made) to the extracellular compartment by a concentration gradient in order to be excreted from the body (see Figure 2d).

4. Extracellular Sub-Compartment C_n Concentrations Are Equal

Vitamin D metabolite, m_n, concentrations may differ somewhat between extracellular sub-compartments/spaces and their concentration gradients around cells may vary. However, in our model, the concentrations of $25(OH)D_3$ and its many metabolites (including $1,25(OH)_2$ D_3) are assumed to be uniform for the same metabolites across different extracellular sub-compartments at any given point in time.

5. Nanomoles, 10^{-9} Moles (nmols) of Active Vitamin D Synthesized over 24 h Equals the nmols of Active Vitamin D End Metabolites Synthesized over the Same 24 h

The Molar Balance Model for active vitamin D synthesis assumes that the number of nmols of active vitamin D synthesized over a 24 h period equals the sum of the number of nmols of end metabolites of active vitamin D synthesized over the same 24 h. This steady state assumption further depends on the following: (1) any change in the total body's number of nmols of active vitamin D or in the number of nmols of active vitamin D intermediate metabolites in the intracellular plus extracellular compartments is small compared to the synthesis of active vitamin D end metabolites over 24 h, and (2) the number of nmols of active vitamin D and active vitamin D intermediate metabolites excreted is relatively small compared to the nmols of end metabolites excreted over the same 24 h period. All the measurements made using this and the following assumptions are in units of nmols. The fact that this measurement is made over 24 h allows this measurement also to represent active vitamin D synthesis per 24 h (a synthesis rate).

The equations derived to determine the nmols of active vitamin D synthesized over 24 h depend on the above assumptions. The validity of these assumptions could be checked by doing second serum and urine assays which measures total end metabolites of active vitamin D precursor, active vitamin D, and all their intermediate metabolites after all active vitamin D precursor, active vitamin D, and its intermediate metabolites are driven to their end metabolites by adding significant excess CYP24A1 hydroxylase enzyme. If,

after adding measured nmols of serum active vitamin D and its precursor, 25(OH)D_3, to the measurement of their end metabolites in the first sample, a discrepancy between the sum of these metabolites in the first sample and the total end metabolites of 25(OH)D_3 and 1,25$(OH)_2D_3$ in the second sample exists, then a correction factor can be added to the calculation (see further discussions below and in the Appendix A, Section 2, Assumptions).

6. The nmols of End Metabolites, $m_{8:10}$, in the Intracellular plus Extracellular Spaces Can Be Used to Estimate the nmols of Active Vitamin D Synthesis (Levels) at Time (t).

The total nmols of active vitamin D, 1,25$(OH)_2D_3$ end metabolites (m_8, m_9, and m_{10}) in the extracellular plus intracellular spaces, can be used to estimate the body's total active vitamin D synthesis at any point in time, (t). The assumption in the sentence above allows for a quicker method for assessing active vitamin D synthesis at any given time (t) from a single plasma sample and to track changes in active vitamin D synthesis due to exogenous vitamin D supplementation. The use of only the end metabolites of active vitamin D as a biomarker for active vitamin D synthesis only approximates active vitamin D synthesis when the levels (synthesis) of active vitamin D and its intermediate metabolites are changing significantly (going up or down) as the demand and synthesis of active vitamin D changes.

As with the 24 h assessment above, a second plasma serum assay could be performed which measures the total end metabolites of active vitamin D after all active vitamin D and its intermediate metabolites are driven to their end metabolites by the CYP24A1 hydroxylase enzyme. This assay could be used to check for a significant buildup of active vitamin D intermediate metabolites relative to active vitamin D end metabolites. If the discrepancy is large then a factor to correct for this discrepancy must be added to the molar balance model calculation. This same analysis could be performed on a spot urine although the dilution variability of spot urines would have to be accounted for (see Figure 2a,b and Assumptions (A.8) and (A.9) and their description in Appendix A).

7. The Total End Metabolites of 25(OH)D_3 in the Extracellular and Intracellular Spaces That Are Not Metabolized from 1,25$(OH)_2D_3$ Represent the nmols of Vitamin D precursor, 25(OH), That Are Diverted away from the Synthesis of Active Vitamin D at Any Point in Time (t)

Determination of the total nmols of m_6 and m_7 (end metabolites of m_0) in the extracellular and intracellular spaces at time (t) are assumed to represent the total number of nmols of 25(OH)D_3 diverted away from the synthesis of active vitamin D at time (t). This assumption further assumes that the nmols of diverted 25(OH)D_3 (m_0) intermediate metabolites are small in number compared to the end metabolites of diverted 25(OH)D_3 (m_0). The assumption in the sentence above allows for a quicker method (1) to assess the total nmols of vitamin D precursor, 25(OH)D_3 diverted away from the synthesis of active vitamin D at any given time (t) from a single plasma sample and (2) to track changes in active vitamin D precursor diversion following exogenous vitamin D supplementation.

The validity of this assumption can be checked by doing a second serum assay from a plasma sample drawn at time (t) which measures total end metabolites of active vitamin D precursor, m_0, after 25(OH) vitamin D and all active vitamin D precursor intermediate metabolites are driven to their end metabolites by CYP24A1 hydroxylase enzyme. In this case, the number of nmols of active vitamin D precursor, m_0, originally in the serum level of the plasma sample must be subtracted from the measured diverted end metabolites of m_0. The diverted nmols of active vitamin D are used in the calculation of the active vitamin D demand ratio and in the determination of the percent utilization of active vitamin D precursor, m_0, in the synthesis of active vitamin D.

8. This Model Assumes That 25% of 1,25$(OH)_2D_3$ and Its Metabolites Are Excreted in the Urine and 75% Are Excreted in the Stool from Bile (See further explanation in 3. Results S text below)

3. Results

Model Derivation through Figures and Equations

Based on the above assumptions, Figure 2a–d, and Tables 1 and 2 in this paper and the following equations in this paper (including in the Appendix A), the synthesis of and demand for $1,25(OH)_2D_3$ by the many cells/tissues of the body is estimated, and the percent utilization of vitamin D_3 precursor, 25(OH)D for the synthesis of active vitamin D by the body is determined. Finding a way to estimate the nmols of intracellular $1,25(OH)_2D_3$ synthesized in the body at any point in time (t) or over a period ($t_1 - t_0$) such as 24 h (in nmols) could be used to identify changing demand for $1,25(OH)_2D_3$. Determination of the change in total end inactive metabolites of $1,25(OH)_2D_3$ in the extracellular and intracellular compartments of the body over 24 h (in nmols), plus the number of nmols of $1,25(OH)_2D_3$ end inactive metabolites excreted over the same 24 h period, provides a way to estimate the 24 h synthesis of intracellular $1,25(OH)_2D_3$.

Measurement of the nmols of the end inactive metabolites of $1,25(OH)_2D_3$ excreted from the body in bile/stool during a 24 h period would be difficult. However, an estimate can be made by measuring the end inactive metabolites in a 24 h urine sample and then correcting for the number of inactive metabolites excreted by the stool. Based on previous studies, this model uses the estimation that 25% of $1,25(OH)_2D_3$ end metabolites are excreted in the urine and 75% are excreted in the stool from bile [41–43].

Measuring the nmols of all the intermediate and end metabolites of $1,25(OH)_2D_3$ in a plasma specimen or in a 24 h urine collection would be tedious. However, measurement of the nmols of the three primary end metabolites of $1,25(OH)_2D_3$ (i.e., 1-OH-23-COOH-24,25,26,27 Tetranor D_3 or calcitroic acid, $1,25R(OH)_2D_3$-26,23S-lactone or calcitriol-26,23-lactone, and 23-COOH-24,25,26,27 Tetranor D_3 or Calcioic acid) in a plasma specimen and in a 24 h urine may allow the approximate determination of active vitamin D, $1,25(OH)_2D_3$, synthesis. This approximation might be achieved by utilizing the 25% excretion in the urine assumption and the other assumptions listed above (See also the Appendix A).

Since only 25% of the actual excretion of these three vitamin D end metabolites from the body occurs through the urine, the total excretion of end inactive vitamin D metabolites from the body during the 24 h period is four times the excretion in urine. A finding of changing excretion quantities of $1,25(OH)D_3$ end metabolites over 24 h occurring at the same plasma $25(OH)D_3$ concentration in the same individual under different conditions (where the body requires higher or lower amounts of active vitamin D) would support one of the assumptions of this model. Namely, the excretion of fluctuating inactive end metabolites of active vitamin D (and by inference fluctuating active vitamin D synthesis) in the body exists which is partially independent of extracellular plasma active vitamin D precursor $25(OH)D_3$ levels.

The small letter m and its subscripts n (0–10) are used to identify specific metabolites in the vitamin D synthesis pathway. Figure 2a,b describe the enzyme pathways that metabolize $25(OH)D_3$, m_0, into the production of active vitamin D hormone, $1,25(OH)_2D_3$, m_1, and its metabolites. The enzyme pathways that metabolize m_0 away from the synthesis of active vitamin D into inactive metabolites are part of the body's regulation of the synthesis of active vitamin D and are also described in Figure 2a,b (see yellow oval).

Figure 2a diagrams some of the intracellular compartment's enzymatic reactions which result in the accumulation of initial and end metabolites of $25(OH)D_3$ over some arbitrary time interval ($t_1 - t_0$) in nmols. Figure 2b diagrams the rate of synthesis in the intracellular compartment of initial and end metabolites of $25(OH)D_3$, ($S_{0,n}$) in units of nmols/t. Figure 2c presents a simplified diagram of the synthesis, transport of vitamin D metabolites between the intracellular and extracellular compartments, and excretion of vitamin D precursor, active vitamin D, and their end metabolites. Shown with Figure 2c are previously measured extracellular, plasma, and intracellular compartment volumes for an average male and female.

Unlike Figure 1 which describes both the front and backends of the vitamin D metabolic pathways, Figure 2c,d. describe the backend of the vitamin D metabolic path-

ways. Figure 2d presents a simpler diagram of the synthesis of the end metabolites of $25(OH)D_3$ and $1,25(OH)_2D_3$ which are produced in some cells/tissues of the body which contain the CYP24A1 enzyme. This enzyme controls the breakdown of active vitamin D, $1,25(OH)D_3$ and the portion of active vitamin D precursor, $25(OH)D_3$, which is diverted away from the synthesis of active vitamin D (See Figure 2a,b). The cells/tissues in diagram, Figure 2d, have arrows pointing out of the cells/tissues to indicate these cell's ability to metabolize $25(OH)D_3$ and $1,25(OH)_2D_3$ by the ubiquitous enzyme, CYP24A1. The greater the size of the arrow leaving the cell indicates the greater the concentration of CYP24A1 RNA in the cell, the greater the potential of the cell to synthesize the CYP24A1 enzyme, and ultimately the greater the ability of the cell to metabolize $25(OH)D_3$ and $1,25(OH)_2D_3$ to their end metabolites.

The pathways from the active vitamin D precursor, $25(OH)D_3$, allow the body to match the synthesis of active vitamin D_3 to the body's demand for $1,25(OH)_2D_3$. If sufficient or more than sufficient vitamin D precursor exists to meet the body's demand for $1,25(OH)_2D_3$, then the excess can be diverted away from the synthesis of active vitamin D. In Figure 2d, the red + signs represent the end inactive metabolites of active vitamin D, $1,25(OH)_2D_3$, or m_1 and the blue + signs represent the end inactive metabolites of the vitamin D precursor, $25(OH)D_3$, or m_0 that are diverted away from the synthesis of active vitamin D. The arrows in Figure 2d represent the flow of the end metabolites of $25(OH)D_3$ and $1,25(OH)_2D_3$ between the intracellular space where these metabolites are synthesized and the extracellular space from which they are secreted into the urine and stool. The flow is assumed to be driven by a concentration gradient (high to low). The size of the arrows represents the quantity of CYP24A1 RNA in the cells/tissues.

Concepts developed in Figure 2a–d. are used to develop formulas in the Appendix A to estimate the amount of active vitamin synthesized by the body through measurement of the total end metabolites of $1,25(OH)_2D_3$. The equations listed in this text are numbered as they are in the Appendix A where they were derived. The integral of $S_{0,1}$, expressed in Equations (1) and (2) from the Appendix A and repeated below, represents the amount of $1,25(OH)_2D_3$ produced by cells/tissues of the body over a time interval $(t_1 - t_0)$. This integral of $S_{0,1}$ can also be used to estimate the amount of active vitamin D that has been synthesized in the body at any time (t). See Appendix A, Equations (9a), (10a) and (13a). One formula uses the integral of the rate of active vitamin D synthesis, $(S_{0,1})$ over an arbitrary 24 h time interval to estimate the total synthesis of $1,25(OH)_2D_3$ over 24 h. This synthesis estimate is accomplished by summing the change in the total amount of the end metabolites of $1,25(OH)_2D_3$ in the extracellular and intracellular compartments and the accumulation of end metabolites of $1,25(OH)_{2r}D_3$ in urine and stool over 24 h.

So far, this method has focused on the use of the end metabolites of active vitamin D and the end metabolites of its precursor, $25(OH)D_3$ (which are formed from vitamin D precursor which is diverted away from the synthesis of active vitamin D) in order to evaluate the actual amount of and the need for active vitamin D synthesis. There is one other consideration concerning the synthesis of active vitamin D and the serum concentration of active vitamin D precursor. Gene CYP27B1 of enzyme C1 Hydroxylase is responsible for the synthesis of active vitamin D from its precursor (see Figure 2a and the yellow oval, Figure 2b) and the gene CYP2R1 is responsible for the synthesis of active vitamin D precursor, $25(OH)D_3$, from D_3. When these genes become mutated and are no longer able to produce functioning 1-α Hydroxylase or 25-hydroxylase enzymes, respectively, severe active vitamin D deficiency can occur [47].

There may be some genetically variable forms of these deficiencies which may impair the production of their hydroxylase enzymes and effect the production of active vitamin D or its precursor without totally stopping the production of these forms of vitamin D. Measurement of the end metabolites of active vitamin D, of its precursor, $25(OH)D_3$, and of the end metabolites of diverted active vitamin D precursor, may help to determine whether either of these two genes and the production rate of their enzymes may be altered.

A second formula has been derived to determine $M_1(t)$ (Equation (3) below) or the amount of end metabolites of active vitamin D, m_1, that are present in the body at any point in time (t). The amount of end metabolites of active vitamin D in the body at time (t) is then assumed to represent or to be proportional to the amount of active vitamin D synthesized at that moment. The following numbered equations are taken from derivation of equations in Appendix A that quantify active vitamin D synthesis and demand as well as the percent utilization of the precursor to active vitamin D for active vitamin D synthesis.

$$\int_{t_0}^{t_1} S_{0,1(t)}\, dt = 4.66\mathrm{Vp}[(2\beta)+1] \times [C_{8,p}(t_0, t_1) + C_{9,p}(t_0, t_1) + C_{10,p}(t_0, t_1)] + 4[C_{8:10,u}(t_1)\mathrm{Vu}(t_1)] \quad \text{(Eq. 1)}$$

for men where V_p = 3.0 L, $V_u(t_0) = 0$, and β is initially set at 1.1 (Appendix A)

$$\int_{t_0}^{t_1} S_{0,1(t)}\, dt = 4.4\mathrm{Vp}\ [(2\beta)+1] \times [C_{8:10,cp}(t_1, t_0)] + 4[C_{8:10,u}(t_1)\mathrm{Vu}(t_1)] \quad \text{(Eq. 2)}$$

for women where V_p = 2.5 L, $V_u(t_0) = 0$, and β is initially set at 1.1 and

$$M_1(t) = M_{8:10}(t) = \beta C_{8:10,cp}(t) 2V_e + C_{8:10,cp}(t)V_e \quad \text{(Eq. 3)}$$

where $V_e = 4.66V_p$ for men and $4.4V_p$ for women and β is set at 1.1

In the Appendix A, formulas for a $1,25(OH)_2D_3$ demand ratio, $Drm_{1,i+e}(t)$, Equation (4) below and a $1,25(OH)_2D_3$ 24 h Urine demand ratio, $Drm_{1,u}(t_0,t_1)$, Equation (5) below are also derived. The rationale for using the ratio of the end inactive metabolites of $1,25(OH)_2D_3$, m_1, as the numerator and the end inactive metabolites of $25(OH)D_3$, m_0, as the denominator, is that this ratio will decrease if excess $25(OH)D_3$ exists and is shunted away from the synthesis of active vitamin D when the body's active vitamin D supply is adequate and vice versa. Knowing this ratio may be helpful clinically to judge whether there is sufficient vitamin D precursor to meet the needs of the body for active vitamin D synthesis. This concept has been introduced previously based on calculating a serum calcitriol/calcifediol ratio using this ratio as an indicator of vitamin D hydroxylation efficiency or as an indicator of relative vitamin D CYP enzyme activities rather than the actual indirect measurement of actual molar substrate $1,25(OH)_2D_3/25(OH)D_3$ ratios in the body using the end metabolites of active vitamin D and its immediate precursor [40,48] (see p. 641, Figure 37.3 in Ref. [46]).

$$\mathrm{Drm}_{1,i+e}(t) = \frac{M_{8:10,i+e}(t)}{M_{6:7,i+e}(t)} \quad \text{(Eq. 4)}$$

$$\mathrm{Drm}_{1,u}(t) = \frac{M_{8:10,u}(t)}{M_{6:7,u}(t)} \quad \text{(Eq. 5)}$$

An increase in m_1 demand should result in an increase in m_1 synthesis from m_0 accompanied by a decrease in diversion of m_0 away from m_1 synthesis. (i.e., an increase in the m_1 demand ratio) This pattern is suggested in the results of a recent study comparing serum vitamin D metabolites between non pregnant women (controls) and pregnant women (at 15 weeks). One group of pregnant women were without the complication of preeclampsia and one group of pregnant women (at 15 weeks) who went on to develop preeclampsia [23]. As stated above, demand for active vitamin D increases during pregnancy. Mean serum active vitamin D levels, m_1, in these three groups above were, respectively: 85.6, 336.3, and 388.8 pmoles/L. The levels of initial inactive $24,25(OH)_2D_3$, m_2, metabolites of m_0, changed in the opposite direction from active vitamin D synthesis and were, respectively: 9.7, 6.5, and 3.2 nmoles/L These metabolites decreased in parallel with higher m_1 levels. The differences were not statistically significant but the numbers of subjects were small, respectively: 9, 25, and 25.

A somewhat different pattern was seen in urine samples of one of the initial metabolites of active vitamin D precursor, m_0 which was diverted away from the synthesis of active

vitamin D. Mean metabolite m_2, 24,25$(OH)_2D_3$, levels in the urine of these three groups were, respectively: 55.4, 84.1, and 35.6 nmols/liter [23]. The mean m_2 concentrations in the urine samples decreased in the preeclampsia pregnant group compared to the non-preeclampsia pregnant group suggesting higher utilization % in the pre-eclampsia group. The difference between the m_2 levels between the two pregnant groups was statistically significant. Of note, the other initial intermediate metabolite of m_0, 23,25$(OH)D_3$ or m_3 which also diverts m_0 away from the synthesis of active vitamin D was not measurable in the urine samples of this study.

A second method for estimating active vitamin D demand would be determination of the % of vitamin D precursor, 25$(OH)D_3$, m_0, that is used to synthesize active vitamin D, 1,25$(OH)_2$ D_3, m_1, at one point in time (t) or over 24 h. The first % utilization measurement, $Ut_{\%}m_{0,i+e}(t)$, is presented in Equation (6) and represents the percent of m_0 utilized at a single point in time (t) based on the measurements of the end metabolites, $m_{8:10}$ and $m_{6:7}$ in the intracellular and extracellular compartments. The second measurement of m_0 percent utilization presented in Equation (7) is based on the measurement of the change in $m_{8:10}$ and $m_{6:7}$ end metabolites in the intracellular and extracellular compartments over 24 h plus the total amount of $m_{8:10}$ and $m_{6:7}$ end metabolites excreted in the same 24 h. (Recall the total body excretion of end metabolites is equal to 4 × the amount of end metabolites excreted in urine. See Appendix A.

$$Ut\%m_{0,i+e}(t) = \frac{M_{8:10}}{M_{8:10}+M_{6:7}} \times 100\% \quad \text{(Eq. 6)}$$

$$\int_{t_1}^{t_0} U't\%m_0 dt = \frac{\int_{t_0}^{t_1} S_{0,1(t)}\, dt}{\int_{t_0}^{t_1} S_{0,1(t)}\, dt + \int_{t_0}^{t_1} S_{0,6,7(t)}\, dt} \times 100\% \quad \text{(Eq. 7)}$$

4. Discussion

4.1. Measurement of End Metabolites $m_{8:10}$ and $m_{6:7}$

Although the equations above may seem tedious, they will be solved using simple concentration measurements of seven metabolites of vitamin D from plasma and from a 24-h urine sample (including the currently common measurement of plasma m_0, 25$(OH)D_3$ and m_1, 1,25$(OH)_2D_3$). The seven required metabolite concentration measurements include:

m_0—25$(OH)D_3$—precursor of active vitamin D—used now to evaluate vit. D status;
m_1—1,25$(OH)_2D_3$—active vitamin D (currently available);
m_6—25,26,27-Trinorcholecalciferol-24-carboxylic acid—non m_1 inactive end metabolite of m_0.
m_7—25$(OH)D_3$-26-23 Lactone—non m_1 inactive end metabolite of **m_0**;
m_8—1-OH-23-COOH-24,25,26,27 Tetranor D_3—inactive end metabolite of m_1;
m_9—1,25R,$(OH)_2D_3$-26-23S—inactive end metabolite of m_1;
m_{10}—23-COOH-24,25,26,27 Tetranor D_3—inactive end metabolite of m_1.
Note: See Figure 2a,b.

This molar balance approach depends on the accurate and standardized measurement of the serum end metabolites of active vitamin D and of the diverted end metabolites of its precursor, 25$(OH)D_3$. These measurements are the critical foundation of this method. Serum, which is plasma with platelets and clotting factors removed, is used to make these measurements. The serum samples will be formed by spinning down a whole blood sample after clotting has occurred in order to separate the serum from the blood sample cells, platelets, and clotting factors.

Liquid-chromatography-tandem-mass spectrometry (LC-MS-MS) is considered the measurement of choice for vitamin D metabolites [49,50]. With LC-MS-MS, up to twelve vitamin D metabolites have been measured simultaneously [51,52]. Analytical challenges exist with this technology. Sample type, protein precipitation, analyte extraction, derivatization, chromatographic separation ionization, and capabilities of the mass spectrometer

must be addressed [50]. Calibration, standardization, and use of internal standards are also important requirements to achieve consistent, accurate results.

Purified standard compounds for only two of the three end metabolites of active vitamin D, m_8, calcitroic acid, and m_{10}, calcioic acid are available commercially [53–55]. A purified standard compound for the remaining end metabolite of active vitamin D, m_9, or calcitriol-26,23-lactone, and standard compounds for the diverted, m_0 precursor, end metabolites, m_6 or cholacalcioic acid and m_7 or 25(OH)D_3-26-23 lactones will have to be synthesized since these standard compounds are required for the liquid-chromatography-tandem-mass spectrometry measurements of these serum end metabolite measurements.

About 90% of circulating 25(OH)D_3 is protein bound to vitamin D binding protein (VDBP), albumin, and lipoproteins [49]. The percent binding of active vitamin D end metabolites, and the diverted vitamin D precursor end metabolite, to serum VDBP may not be known. The binding of end metabolites and their relative fat and water solubilities may have to be determined. Measurement of the three end metabolites of active vitamin D and the two end metabolites of the precursor, 25(OH)D_3 which are diverted away from the synthesis of active vitamin D, may also depend on their actual concentrations in plasma and urine and the range of measurability. The measurements of these end metabolites would be made using the same instruments that are currently measuring other forms of vitamin D.

A source of human CYP24A1 hydroxylase enzyme will be needed to further evaluate and test the proposed assays used by this model. This enzyme will be used to drive the intermediate metabolites to their end metabolites. This reagent (enzyme) will be required to verify that there is not a significant change in total intermediate metabolites during a transitory increase or decrease in active vitamin D synthesis or in the rate of vitamin D precursor diversion. This enzyme is currently available from several commercial sources Biocompare, "https:www.biocompare.com/Search-Biomolecules/?search=CYP24A1 (accessed on 17 July 2020)" [53]. CYP24A1 has been used in previous vitamin D metabolic studies [54].

Vitamin D metabolite measurements have also been made from human spot urine specimens including 25(OH)D_3 and 24,25$(OH)_2D_3$ [23]. Measurement of human spot urine 1,25$(OH)_2D_3$ and 23,25$(OH)_2D_3$ concentrations were below the limits of detection. The normal volume range of an adult 24 h urine is 800–2000 17mL with a normal intake of 2 L of fluid per day. Since the 24 h urine can be concentrated, concentrating the urine will make the detection of end metabolites in urine easier.

Finally, the technologies used in measuring or monitoring vitamin D metabolites, although challenging, are well established. The only new aspect is adding five different end metabolites of vitamin D to the two currently dominant forms of vitamin D measured, (i.e., active vitamin D_3, 1,25$(OH)_2D_3$ and its immediate precursor, 25(OH)D_3).

4.2. How Can and Why Should These Vitamin D Parameters Be Used?

Using a molar balance model approach, the following vitamin D parameters can be calculated: (1) an estimate of active vitamin D synthesis in the body at any time (t) and over a 24 h time interval, (2) an active vitamin D demand ratio, and (3) an active vitamin D % utilization. Clinical lab software will perform the calculations listed in Equation (9a) through 18 using the measured concentrations of the end metabolites $m_{8:10}$ and $m_{6:7}$ as well as different constants for men and women. Each of these new vitamin D parameters can then be determined and monitored in many different conditions where the demand by the body for active vitamin D changes dramatically. These parameters cannot be currently determined by simply measuring serum 25(OH)D_3 and 1,25$(OH)_2D_3$ levels in the serum.

During severe infections caused by many different agents including the SARS-CoV-2 virus, the immune system may require significantly greater synthesis of active vitamin D to suppress the offending agent (i.e., virus) and the inflammatory response caused by the agent [56]. These clinical vitamin D parameters along with other measurements of an individual's clinical response to their COVID-19 infection will assist clinicians to establish

when significant additional vitamin D supplementation is helpful and to determine the required type and dose of vitamin D supplementation.

4.3. Molar Balance Model Limitations

The molar balance model depends on several assumptions some of which may need modification as the end metabolites are initially measured and some of the assumptions will not be accurate in all situations. If the extracellular volume or plasma volumes change significantly due to swelling, the assumed volume values will have to be modified. Kidney failure will also prevent the measurement of end metabolites in the urine and may lead to build up of some end metabolites in the body including the extracellular compartment and plasma, and lead to greater excretion of these metabolites in the stool.

5. Summary

A new method using a molar balance model is proposed to determine total body active vitamin D, m_1, levels including synthesis over a 24 h period, the level of demand in an individual for active vitamin D, and the % utilization of vitamin D precursor, m_0, to synthesize active vitamin D. Determination of these parameters associated with vitamin D levels and synthesis will require the measurement of the end vitamin D metabolites $m_{6:10}$ in both serum and urine using the same equipment and techniques used to measure active vitamin D and its immediate precursor. Knowing this new information may enable clinicians to improve the body's immune system response to COVID-19 viral infections as well as to other viruses going forward by maximizing the positive effects of active vitamin D on immune system function.

6. Conclusions

(1) Because cells/tissues of the body (especially immune system cells) sometimes have dramatically changing requirements for active vitamin D, there may not be a consistent stored amount of vitamin D (as measured by plasma $25(OH)D_3$ levels) or single minimum daily requirement to insure enough active vitamin D synthesis in all circumstances.

(2) Knowing the total active vitamin D that has been synthesized at one point in time or that has been synthesized over 24 h, knowing the demand ratio for active vitamin D, and knowing the % utilization of $25(OH)D_3$, m_0, for the synthesis of active vitamin D may help us to determine changing requirements for active vitamin D at any given time or in different situations the body may encounter.

(3) Similarly, knowing these vitamin D parameters may improve our understanding of how-to better dose active vitamin D and active vitamin D precursor supplementation.

(4) Suppression of COVID-19 replication or that of another new virus by adequate levels of active vitamin D may not only reduce the effect of the virus on an individual but may also lower the level of contagiousness of an individual with a COVID-19 or other virus infection. Lowering the contagiousness may slow the spread of the virus by lowering the positivity rate within a community [57].

Funding: Salisbury Foundation for Research and Education—Grant # 18-020, Project # 1575420-4, National Association of Veterans' Research and Education Foundations, NAVREF.

Institutional Review Board Statement: Not applicable.

Data Availability Statement: Not Applicable.

Acknowledgments: This paper is based in part upon research supported by the U.S. Department of Veterans Affairs, Research Department, W.G. (Bill) Hefner VA Medical Center, Salisbury, NC. The welfare of human subjects was protected and the W.G. (Bill) Hefner VA Medical Center Institutional Review Board and Research Committee approved all research involving human subjects. (Study: IRB Protocol 18-020—"Medical Evaluation of U.S. Veterans with Chronic Multi-symptom illnesses". Sean R. Maloney is a part-time physician employee of the U.S. Government. This work was prepared as

part of his official duties. Title 17, USC, 105 provides that "Copyright protection under this title is not available for any work of the U.S. Government". Title 17, USC, 101 defines a U.S. Government work as "a work prepared by an employee of the U.S. Government as part of that person's official duties". The following individuals have kindly reviewed this manuscript and added timely and helpful comments improving the content of this paper. In addition, Matthew Maloney verified the calculations used by the model, reviewed the assumptions used by the model and improved the nomenclature/variable symbols used by the model. All the following individuals have agreed to be acknowledged as contributing to this article: Maria E. Ariza; Marshall Williams; Paula Goolkasian; Amitha K. Hewavitharana; Matthew R. Maloney.

Conflicts of Interest: The authors declare no conflict of interest. The views expressed in this paper are solely those of the author and do not reflect those of the Department of Veterans Affairs, the US Government, or any other institution.

Appendix A. Molar Balance Model Derivation

1. Definitions D

1.0. List of Included Vitamin D m_n Metabolites

mD_3—D_3—precursor of **m_0** (Figure 2c only)
m_0—25(OH)D3—precursor of active vitamin D_3
m_1—1,25$(OH)_2D_3$—initial active vitamin D_3 metabolite of **m_0**
m_2—24,25$(OH)_2D_3$—an initial inactive metabolite of **m_0**
m_3—23,25$(OH)_2D_3$—an initial inactive metabolite of **m_0**
m_4—1,24,25$(OH)_3D_3$—an initial inactive metabolite of **m_1**
m_5—1α,23S,25$(OH)_3D_3$—an initial inactive metabolite of **m_1**
m_6—24-COOH-25,26,27 Trinor D_3—non m_1 inactive end metabolite of **m_0**
m_7—25(OH)D_3-26-23 Lactone—non **m_1** inactive end metabolite of **m_0**
m_8—1-OH-23-COOH-24,25,26,27 Tetranor D_3—inactive end metabolite of **m_1**
m_9—1,25R,$(OH)_2D_3$-26-23S—inactive end metabolite of **m_1**
m_{10}—23-COOH-24,25,26,27 Tetranor D_3—inactive end metabolite of **m_1**

Note: See Figure 2a,b.

1.1. Metabolite Quantities and Concentrations. The Quantity of Vitamin D Metabolites at Time t Is Denoted

$$m_{n,k}(t), \tag{D.1}$$

where the first subscript, n, indexes metabolite type (see list above for metabolite definitions) and the second subscript, k, designates three dimensional spaces in which metabolites can be located. There are four primary spaces or compartments: intracellular, extracellular, plasma, and collected urine. The plasma space is a sub-compartment of the extracellular space. Two secondary spaces used in the mathematical derivation include the body's stool space and the space or volume of the collected plasma samples used to make metabolite measurements. The spaces are denoted as follows:

(1) k = i for intracellular space
(2) k = e for extracellular space
(3) k = p or pla for plasma sub-extracellular space
(4) k = u collected urine space
(5) k = s collected stool space
(6) k = cp collected plasma sample

Note: number subscripts always refer to metabolites or time and letter subscripts to spaces.

The total body nmols of metabolite m_n at any time (t) in the intracellular and extracellular compartments is denoted:

$$M_{n,i+e}(t) \tag{D.2}$$

The total nmols of metabolite m_n over any time period ($t_1 - t_0$) in a urine collected specimen is denoted:

$$M_{n,u}(t_1) - M_{n,u}(t_0) = M_{n,u}(t_1) \quad \text{(D.3)}$$

since the nmols at the start of a urine collection will always be = to 0.

Metabolite concentrations in each space are defined as:

$$C_{n,k}(t) = m_n,k(t)/V_k \quad \text{(D.4)}$$

where Vk is the volume in compartment k.

1.2. Metabolite Transport, Synthesis, and Loss

The transport rate of any metabolite n from the intracellular to extracellular compartment (space) at time (t) is

$$R_n(t) \quad \text{(D.5)}$$

We consider several pathways of vitamin D metabolite synthesis and use S to denote rates of synthesis/conversion. All synthesis/conversion occurs in the intracellular compartment. The rate of synthesis/conversion between metabolites i and j, where $i \neq j$, is denoted

$$S_{i,j}(t) \quad \text{(D.6)}$$

Some specific synthesis rates of interest are:

$$S_{0,1}(t)\text{: synthesis rate of metabolite } m_1 \text{ from metabolite } m_0 \quad \text{(D.7)}$$

$$S_{4,8}(t), S_{5,9}(t), \text{ and } S_{5,10}(t)\text{: synthesis rates of the end metabolites of } m_1 \text{ from the first intermediate metabolites of } m_1 \quad \text{(D.8)}$$

$$S_{0,2}(t) + S_{0,3}(t) = S_{0,2:3}(t) \text{ equals the synthesis rate of intermediate metabolites } m_2 + m_3 \ (m_{2:3}) \text{ from metabolite } m_0 \quad \text{(D.9)}$$

Note: $S_{0,2:3}(t)$ denotes synthesis rate of the first intermediate metabolites of m_0 diverted away from the synthesis of active vitamin D, m_1.

$$S_{2,6}(t) \text{ and } S_{3,7}(t)\text{: synthesis rate of the end metabolites of } m_0 \text{ diverted away from the synthesis of } m_1 \quad \text{(D.10)}$$

One goal of this model is to develop a method for measuring the synthesis of the active vitamin D metabolite, m_1. Using our notation, the total quantity of m_1 synthesized from m_0 between two arbitrary time periods t_0 and t_1 is

$$\int_{t_0}^{t_1} S_{0,1(t)}\, dt \quad \text{(D.11)}$$

1.3. Metabolite Loss and Urine Volume Creation

The total loss of metabolite m_n from the extracellular space is divided between the urine volume space, 25% and the stool volume space 75%. Total rate of metabolite, m_n, loss:

$$L^*_n(t) = L_{n,u}(t) + L_{n,s}(t) = 4L_{n,u}(t) \quad \text{(D.12)}$$

and we denote the rate of urine volume creation at time t as

$$U(t) \quad \text{(D.13)}$$

The collected urine volume consists of a urine volume created between the time at which collection starts, t_s or t_0, and the time at which collection ends, t_e or t_1. Clinically, the

urine volume is always 0 at the start of a urine collection; therefore, terms involving t_s or t_0 always drop out.

$$V_u(t_1) - V_u(t_0) = V_u(t_1) = \int_{t_0}^{t_1} U(t)^{dt} \text{ since } V_u \text{ at the start of collection is 0} \quad (D.14)$$

The quantity of metabolite m_n in the urine space at the end of the collection period consists of 25% of metabolites m_n excreted from the body between the time at which collection starts, t_s or t_0, and the time at which collection ends, t_e or t_1. (Note: the remaining 75% of metabolite excretion occurs through the stool). Therefore, we can write

$$\begin{gathered} m_{n,u}(t_1) - m_{n,u}(t_0) + m_{n,s}(t_1) - m_{n,s}(t_0) = \int_{t_0}^{t_1} L^*{}_n(t)^{dt} = 4 \int_{t_0}^{t_1} L_{n,u}(t)^{dt} \\ \text{Since } m_{n,u} \text{at the urine collection start time } (t_0) \text{ is 0 and } [m_{n,s}(t_1) - m_{n,s}(t_0)] = \\ 3m_{n,u}(t_1) \text{ then :} \\ m_{n,u}(t_1) + [m_{n,s}(t_1) - m_{n,s}(t_0)] = 4[m_{n,u}(t_1)] = 4 \int_{t_0}^{t_1} L_{n,u}(t)^{dt} \end{gathered} \quad (D.15)$$

The concentration of metabolite n in the urine space at the end of the collection period is also a function of the end collection time only since the nmoles of m_n and urine volume equal 0 at the start of the urine collection (t_0):

$$C_u(t_1) = \frac{m_{n,u}\ (t1\ )}{V_u(t1)} = \frac{\int_{t_0}^{t_1} L_{n,u}(t)dt}{\int_{t_0}^{t_1} U(t)dt} \quad (D.16)$$

1.4. m_1 Demand Ratio

The 1,25(OH)D_3, m_1, demand ratio expresses the ratio of the sum of end inactive metabolites of active vitamin D, 1,25$(OH)_2D_3$, m_1 (i.e., m_8, + m_9, + m_{10}) to the sum of non m_1, end inactive metabolites of 25(OH)D_3 (i.e., m_6 + m_7) in the intracellular plus extracellular compartments at some point in time, (t).

$$Drm_{1,i+e}(t) \quad (D.17)$$

Note: If the sum of m_6 + m_7 in the denominator cannot be measured or if it becomes very small causing the ratio to become very large, then the denominator can become 1×10^{-9} + m_6 + m_7.

1.5. m_0 Percent Utilization

At any point in time (t), the 25(OH)D_3, m_0, percent utilization equals the sum of end inactive metabolites of active vitamin D, 1,25$(OH)_2D_3$, m_1 (i.e., m_8 + m_9 + m_{10}) divided by the sum of the end inactive metabolites of active vitamin D, 1,25$(OH)_2D_3$, m_1 (i.e., m_8 + m_9 + m_{10}) plus the sum of the end inactive metabolites of m_0 (i.e., m_6 + m_7 or the end metabolites that are diverted away from the synthesis of m_1) multiplied by 100%.

$$Ut_{\%}m_{0,i+e}(t) \quad (D.18)$$

The rate of change of m_0 percent utilization is defined as:

$$Ut'_{\%}m_{0,i+e}(t) \quad (D.19)$$

2. Assumptions A

Plasma volumes are somewhat different between men and woman based on different physical sizes (average woman 55 kg and average male 70 kg) and they have slightly different mean hematocrit % (Hct.%) levels (mean for women 40% and mean for men 45.5%). Thus, the average plasma volume for a 55 kg woman is 2.5 L and for an average 70 kg male 3.0 L. An average male's plasma volume is thus 20% greater than a women's plasma volume. See Figure 2c for more detailed explanation of volume determinations.

For the purpose of this model, the plasma, extracellular, and intracellular volumes are assumed to be known constants for the average female 155 kg and the average male 170 kg, denoted as V_{pla}, V_e, and V_i. The intracellular and extracellular volumes can be expressed as multiples of the plasma volume [29,30]:

$$V_{pla} = \text{constant} = 3.0 \text{ L for men and } 2.5 \text{ L for women} \quad (A.1)$$

$$V_e = \text{constant} = 4{:}66V_{pla} \text{ for men and } 4.4V_p \text{ for women} \quad (A.2)$$

$$Vi = \text{constant} = 9.32V_{pla} \text{ for men and } 8.8V_p \text{ for women} \quad (A.3)$$

For this model, the total nmols of vitamin D metabolites, m_n, in the intracellular and extracellular compartments or spaces will be determined from measurement of metabolite m_n concentrations in a collected plasma sample.

The next assumption is that metabolite concentrations of m_n in the extracellular, plasma, and collected plasma sample are equal at the time (t) of specimen collection, i.e.,

$$C_{n,e}(t) = C_{n,p}(t) = C_{n,cp}(t) \quad (A.4)$$

Mean metabolite concentrations in the intracellular and extracellular compartments are assumed to be proportional with a constant of proportionality of β. β equilibrates the mean concentrations of m_n metabolites between the non-homogeneous intracellular and assumed approximately homogeneous extracellular compartments. End metabolites of m_0 and m_1 are assumed to transfer passively from the intracellular to the extracellular compartment and visa versa passively depending on concentration gradients. β is assumed to be a constant over physiological concentrations of end metabolites, m_n, and to be somewhat greater than 1 since a mean higher to lower concentration gradient overall between the intracellular and extracellular spaces must exist in order for the end metabolites to be excreted from the body. Initially β will be assumed to be 1.1—see Figure 2d.

$$C_{n,i}(t) = \beta C_{n,e}(t) \text{ and therefore} \quad (A.5)$$

$$C_{8:10,i}(t) = \beta C_{8:10,e}(t) = \beta C_{8:10,cp}(t) \text{ and} \quad (A.6)$$

$$C_{6:7,i}(t) = \beta C_{6:7,e}(t) = \beta C_{6:7,cp}(t) \quad (A.7)$$

Assumption A.8 below assumes that the rate of synthesis of m_1 from m_0 is the same as the sum of the rates of synthesis of its three end metabolites. That is, every time 12 molecules of m_1 are synthesized a total of 12 molecules of end metabolites of m_1, $(m_8 + m_9 + m_{10})$, will also be synthesized. Similarly, A.9 assumes that the sum of the rates of synthesis of m_2 from m_0 and m_3 from m_0 is the same as the sum of the rates of synthesis of m_6 from m_2 and m_7 from m_3

$$S_{0,1}(t) = S_{4,8}(t) + S_{5,9}(t) + S_{5,10}(t) \quad (A.8)$$

$$S_{0,2:3}(t) = S_{2,6}(t) + S_{3,7}(t) \quad (A.9)$$

Assumptions A.8 and A.9 do not reflect what is truly going on in the two intracellular vitamin D m_0 pathways because these assumptions neglect possible changing concentration levels and the presence of changing nmols of m_n intermediate metabolites. Assumption A.8 assumes that the rate of active vitamin D synthesis equals the sum of the rate of end metabolite synthesis (a presumed steady state) without a buildup or decrease in intermediate metabolites. Assumption A.9 likewise assumes that the rate of m_0 diversion away from active vitamin D synthesis equals the sum of the rate of its end metabolite synthesis (a presumed steady state) without a buildup or decrease in its intermediate metabolites. Even under non steady state conditions, these two assumptions might introduce a tolerable error.

The validity of A.8 and A.9 assumptions can be checked by doing second serum and urine assays which measures total end metabolites of active vitamin D precursor, active

vitamin D, and all of their intermediate metabolites after all active vitamin D precursor, active vitamin D, and its intermediate metabolites are driven to their end metabolites by excess CYP24A1 hydroxylase enzyme added to a second plasma sample drawn at time t_0 and t_1 as well as by a second determination from the urine specimen collected over 24 h. If, after subtracting out the end metabolites which would have been generated by the remaining active vitamin D and its precursor in the first sample, the measured nmoles of end metabolite in the second sample are significantly larger than those in the first serum sample, then a correction factor can be added to the calculation to account for a buildup of intermediate metabolites in either the 25(OH)D_3 or 1,25$(OH)_2D_3$ degradation pathways when the synthesis of active vitamin D increases.

The collected serum plasma sample can be divided into two equal parts. In the first part, concentrations of $\mathbf{C_{0,cp}(t)}$ (where the subscript 0 indicates 25(OH)D_3 and cp indicates collected plasma) and $\mathbf{C_{1,cp}}$ **(t)** (where the subscript 1 indicates 25$(OH)_2D_3$) of the first collected plasma specimen must be measured along with the concentrations of the end metabolites of 1,25$(OH)_2$, D_3 ($m_{8–10}$) and 25(OH)D_3 ($m_{6–7}$). To the second sample, excess CYP24A1 hydroxylase enzyme is added to completely drive the breakdown of 25(OH)D_3 and1,25$(OH)_2D_3$ to their end metabolites.

Then, measured concentrations of $C_{0,cp}$, $C_{1,cp}$, $C_{6–7,cp}$, and $C_{8–10,cp}$ in the first sample must be subtracted from the concentration of $C_{6:7,cp}(t)$ plus $C_{8:10,cp}(t)$ in the second sample. Any discrepancy between the two values will represent the concentration of intermediate metabolites not measured in the first collected plasma sample. If the discrepancy is significant a correction factor can be introduced to correct for an increase in intermediate metabolites in the 25(OH)D_3 and 25$(OH)_2D_3$ degradation pathways when the synthesis of either of these vitamin D forms increases significantly. The same assumptions and processes described in this and the above paragraphs can be used in the evaluation of the end metabolites of active vitamin D and its precursor in urine collections. This two-measurement comparison technique along with the following equations could be used to see whether the assumption that the buildup of intermediates in these two degradation pathways is not significant or needs addressing.

3. Equations E

3.1. Measurement of Active Vitamin D (m_1) Synthesis and of Vitamin D Precursor (m_0) Diversion away from Active Vitamin D Synthesis over Time Interval ($t_1 - t_0$)

From Assumptions (A.1) to A.10, total m_1 synthesis and the total diversion of m_0 away from the synthesis of active vitamin D, m_1, over an arbitrary time interval ($t_1 - t_0$) can be estimated in men or women using the

(1) Measurement of $C_{8:10,cp}$ at times t_0 and t_1
(2) Measurement of $C_{6:7,cp}$ at times t_0 and t_1
(3) Measurement of $C_{8:10,u}$ at time t_1 (since there is no urine when the collection starts)
(4) Measurement of $C_{6:7,u}$ at time t_1 (since there is no urine when the collection starts)
(5) Measurement of $V_u(t_1)$
(6) Measurement of $C_{0,cp}$ at times t_0 and t_1 and
(7) Standard values for V_i, V_e, and $V_{pla,}$ for men and women.

An expression for the synthesis of m_1 over an arbitrary time interval ($t_1 - t_0$) is developed in three steps. In the first step, an expression for the change in quantity of m_1 in the body's intracellular and extracellular compartments over the time interval, ($t_1 - t_0$) is derived using m_1's end metabolites, $m_{8:10}$. In the second step, an expression for the quantity of m_1 excreted or lost to the body in urine and stool over the same time interval is derived using m_1's end metabolites, $m_{8:10}$. In the third step, the expressions derived in parts 1 and 2 are summed to solve for the total synthesis of active vitamin D, m_1, based on the assumption that the change in intracellular plus extracellular nmols of $m_{8:10}$ over the time interval, plus the loss of $m_{8:10}$ in the urine and stool over the same time interval will represent a good estimate of the synthesis of m_1 over this time interval. Using

the same approach, an expression for the amount of m_0 diverted away from the synthesis of m_1 will be developed using the end metabolites, $m_{6:7}$.

Using Assumption A.8, the following equations can be written:

$$\int_{t_0}^{t_1} S_{0,1(t)}\, dt = \int_{t_0}^{t_1} S_{4,8(t)}\, dt + \int_{t_0}^{t_1} S_{5,9(t)}\, dt + \int_{t_0}^{t_1} S_{5,10(t)}\, dt \quad \text{(Eq. 1a)}$$

$$\int_{t_0}^{t_1} S_{0,1(t)}\, dt = m_{8:10,i}\,(t_1) - m_{8:10,i}\,(t_0) + \int_{t_0}^{t_1} R_{8,10(t)}\, dt \quad \text{(Eq. 2a)}$$

Using Definition (D15), the total change in metabolites m_8, $m_{9,}$ and m_{10} in the extracellular space over the time interval $(t_1 - t_0)$ is

$$m_{8:10,e}(t_1) - m_{0,8:10,e}(t_0) = \int_{t_0}^{t_1} R_{8,10(t)}\, dt - \int_{t_0}^{t_1} L{*}_{8,10(t)}\, dt = \int_{t_0}^{t_1} R_{8,10(t)}\, dt - 4\int_{t_0}^{t_1} L_{8,10(t)}\, dt \quad \text{(Eq. 3a)}$$

Equation (3a) can then be rearranged to solve for the total transfer of metabolites, m_8, m_9, and m_{10} from the intracellular to the extracellular space over the time interval $(t_1 - t_0)$.

$$\int_{t_0}^{t_1} R_{8,10(t)}\, dt = m8:10,e\,(t1) - m8:10,e\,(t0) + 4\int_{t_0}^{t_1} L_{8,10(t)}\, dt \quad \text{(Eq. 4a)}$$

Substituting the above expression for the total transfer (R) back into equation 2 gives:

$$\int_{t_0}^{t_1} S_{0,1(t)}\, dt = m8:10,i\,(t1) - m8:10,i\,(t0) + m0,8:10,e\,(t1) - m0,8:10,e\,(t0) + 4\int_{t_0}^{t_1} L_{8,10(t)}\, dt \quad \text{(Eq. 5a)}$$

The terms on the righthand side of Equation 5a will be replaced with known quantities (either from quantities that have been measured before such as volumes or from measurements that we can make based on our definitions or assumptions). The first substitution will be for the metabolite loss term involving urine. Note time subscripts s for start and e for end have been replaced by 0 for the initial start of the collection where the urine volume and end metabolites of m_1 would be 0 and e would be replaced by 1 at the end time of the collection. (i.e., $t_s = t_0$ and $t_e = t_1$). Using definitions (D15) and (D16), the total loss of metabolites m_8, m_9, and m_{10} from the body between t_0 and t_1 (using a factor four times the loss from urine to make up for the loss of metabolites from both urine and stool equals:

$$4\int_{t_0}^{t_1} L_{8:10,u}(t)dt = 4[m_{8:10,u}(t_1)] = 4[C_{8:10,u}(t_1)V_u(t_1) \quad \text{(Eq. 6a)}$$

Substituting the expression on the righthand side of Equation (Eq.6a) for the metabolite loss term in Equation (Eq.5a) gives:

$$\int_{t_0}^{t_1} S_{0,1}(t)dt = m_{8:10,i}\,(t_1) - m_{8:10,i}\,(t_0) + m_{8:10,e}\,(t_1) - m_{8:10,e}\,(t_0) + 4[C_{8:10,u}(t_1)V_u(t_1)] \quad \text{(Eq. 7a)}$$

The next step is to determine the expression, $m_{8:10,i}\,(t_1) - m_{8:10,i}\,(t_0) + m_{8:10,e}\,(t_1) - m_{8:10,e}\,(t_0)$ in terms of measurable concentrations of $m_{8:10,cp}$ at time (t) and then substitute the new derived expression into the right side of Equation (Eq.7a).

Note: $m_{8:10} = m_8 + m_9 + m_{10}$. Then, using Assumptions A.1–A.5, for men

$$
\begin{gathered}
m_{8:10,i}(t_1) - m_{8:10,i}(t_0) + m_{8:10,e}(t_1) - m_{8:10,e}(t_0) = \\
\frac{\beta[m_{8,p}(t_1) + m_{9,p}(t_1) + m_{10,p}(t_1)] \text{ x } 9.32V_p}{V_p} - \frac{\beta[m_{8,p}(t_0) + m_{9,p}(t_0) + m_{10,p}(0)] \text{ x } 9.32V_p}{V_p} \\
+ \\
\frac{[m_{8,p}(t_1) + m_{9,p}(t_1) + m_{10,p}(t_1)] \text{ x } 4.66V_p}{V_p} - \frac{[m_{8,p}(t_0) + m_{9,p}(t_0) + m_{10,p}(0)] \text{ x } 4.66V_p}{V_p} \\
\text{equals} \\
\frac{2\beta[m_{8,p}(t_1) + m_{9,p}(t_1) + m_{10,p}(t_1)] \text{ x } 4.66V_p}{V_p} - \frac{2\beta[m_{8,p}(t_0) + m_{9,p}(t_0) + m_{10,p}(0)] \text{ x } 4.66V_p}{V_p} \\
+ \\
\frac{[m_{8,p}(t_1) + m_{9,p}(t_1) + m_{10,p}(t_1)] \text{ x } 4.66V_p}{V_p} - \frac{[m_{8,p}(t_0) + m_{9,p}(t_0) + m_{10,p}(0)] \text{ x } 4.66V_p}{V_p} \\
\text{equals} \\
\frac{[(2\beta)+1] \times [m_{8,p}(t_1) + m_{9,p}(t_1) + m_{10,p}(t_1) - m_{8,p}(t_0) + m_{9,p}(t_0) + m_{10,p}(0)] \text{ x } 4.66V_p}{V_p} \\
\text{and thus} \\
m_{8:10,i}(t_1) - m_{8:10,i}(t_0) + m_{8:10,e}(t_1) - m_{8:10,e}(t_0) = [(2\beta)+1] \times [C_{8:10,p}(t_1) - C_{8:10,p}(t_0)] \times 4.66V_p \\
\text{where} C_{8:10,p}(t) = C_{8,p}(t) + C_{9,p}(t) + C_{10,p}(t) \cdots\cdots \text{nmoles/L}
\end{gathered}
\tag{Eq. 8a}
$$

substituting the right side of Equation (8a) into the right side of Equation (7a) (for men) results in:

$$
\begin{gathered}
\int_{t_0}^{t_1} S_{0,1(t)}\, dt = [(2\beta)+1] \times [C_{8:10,p}(t_1) - C_{8:10,p}(t_0)] \times 4.66V_p + 4[C_{8:10,u}(t_1)V_u(t_1)\} \\
= 4.66V_p[(2\beta)+1] \times [C_{8:10,cp}(t_1) - C_{8:10,cp}(t_0)] + 4[C_{8:10,u}(t_1)V_u(t_1)]
\end{gathered}
\tag{Eq. 9a}
$$

where V_p for an average size man is 3.0 L, $V_u(t_0) = 0$, and $\beta = 1.1$

For women,

$$
\int_{t_0}^{t_1} S_{0,1(t)}\, dt = 4.4V_p\, [(2\beta)+1] \times [C_{8:10,cp}(t_1) - C_{8:10,cp}(t_0)] + 4[C_{8:10,u}(t_1)V_u(t_1)] \tag{Eq. 10a}
$$

where V_p for an average size woman is 2.5 L, $V_u(t_0) = 0$, and $\beta = 1.1$.

Similarly, for $\int_{t_0}^{t_1} S_{0,2,3(t)}\, dt$ or the amount of m_0 that bypasses the synthesis of m_1. Using the same method

$$
= 4.66V_p\, [(2\beta)+1] \times [C_{6:7,cp}(t_1) - C_{6:7,cp}(t_0)] + 4[C_{6:7,u}(t_1)V_u(t_1)] \tag{Eq. 11a}
$$

where V_p for an average size man is 3.0 L and $\beta = 1.1$.

or

$$
= 4.4V_p\, [(2\beta)+1] \times [C_{6:7,cp}(t_1) - C_{6:7,cp}(t_0)] + 4[C_{6:7,u}(t_1)V_u(t_1)] \tag{Eq. 12a}
$$

where V_p for an average size woman is 2.5 L and $\beta = 1.1$.

3.2. The m_1 Demand Ratio

At any point in time (t), the 1,25(OH)D_3, m_1, demand ratio ($D_{r,i+e}$), expresses the ratio of the sum of end inactive metabolites of active vitamin D, 1,25$(OH)_2D_3$, m_1 (i.e., $m_8 + m_9 + m_{10}$) to the sum of non m_1, end inactive metabolites of 25(OH)D_3 (i.e., $m_6 + m_7$) in the intracellular plus extracellular compartments. The end inactive metabolites of 1,25$(OH)_2D_3$ track the portion of 25(OH)D_3 that goes on to make active vitamin D, m_1. The non m_1 end inactive metabolites of 25(OH)D_3 track the portion of 25(OH)D_3 that is diverted away from making active vitamin D especially when the supply of active vitamin D is sufficient or in excess. See Figure 2a,b and expressions below from Appendix A. This ratio may reflect the body's demand for active vitamin D.

The total body nmols of metabolite m_n at any time (t) in the intracellular and extracellular compartments is denoted:

$$
M_{n,i+e}(t) \tag{D.2}
$$

The quantity (nmols) of active vitamin D, (m_1), or M_1 in the extracellular plus intracellular compartments at time (t) that has been synthesized can then be estimated using the

assumed (A.8) steady state synthesis pathways, [i.e., $S_{0,1}(t) = S_{4,8}(t) + S_{5,9}(t) + S_{5,10}(t)$] and by using the assumptions A.4 and A.5_1 (i.e., the relationship between the mean intracellular compartment $m_{8:10}$ concentrations and the extracellular compartment $m_{8:10}$ concentrations):

$$C_{8:10,i}(t) = \beta C_{8:10,e}(t) = \beta C_{8:10,cp}(t) \quad (A.5_1)$$

The nmols of m_1 in the intracellular plus extracellular compartments at time (t) can then be estimated to equal the nmols of $m_{8:10}$ in the intracellular plus the extracellular compartments:

$$M_{8:10}(t) = \beta C_{8:10,cp}(t)2V_e + C_{8:10,cp}(t)V_e \quad \text{(Eq. 13a)}$$

Similarly, by using (A.9) and substituting $C_{6,7,cp}(t)$ into Equation (Eq.13a), the nmols of m_0 in the intracellular plus extracellular compartments diverted away from active vitamin D synthesis in nmoles can be estimated.

$$M_{6:7}(t) = \beta C_{6:7,cp}(t)2V_e + C_{6:7,cp}(t)V_e \quad \text{(Eq. 14a)}$$

Equations (Eq.13a) and (Eq.14a) represent synthesized nmoles of $m_{8:10}(t)$ and $m_{6:7}(t)$ in the body excluding those metabolites excreted in urine or stool at time (t). See Figure 2a,b.

Based on total intracellular and extracellular nmoles of end metabolites, $m_{8:10}$ and $m_{6:7}$ at time (t), the demand ratio of synthesized active vitamin D to vitamin D precursor diverted away from active vitamin D synthesis would be:

$$Drm_{1,i+e}(t) = \frac{M_{8:10,i+e}(t)}{M_{6:7,i+e}(t)} \quad \text{(Eq. 15a)}$$

When the nmols of intracellular plus extracellular end inactive metabolites ($m_{8:10}$) of active vitamin D increase relative to the nmols of the two end inactive metabolites ($m_{6:7}$) of vitamin D precursor, m_0, the increase in $Drm_{1,i+e}(t)$ may reflect upregulation of the production of $1,25(OH)_2D_3$ from $25(OH)D_3$ (i.e., upregulation of the C1 hydroxylase, CYP27B1 enzyme pathway and increased demand). When $Drm_{1,i+e}(t)$ decreases, the converse may be true (Figure 37.3 in Ref. [30]). Again if the denominator becomes too small or cannot be measured, a factor of 1×10^{-9} can be added to the denominator to prevent the demand ratio from blowing up in size.

Similarly, based on total urine nmoles of end metabolites, $m_{8:10}$ and $m_{6:7}$, the demand ratio of synthesized active vitamin D to vitamin D precursor diverted away from active vitamin D synthesis would be:

$$Drm_{1,u}(t) = \frac{M_{8:10,u}(t)}{M_{6:7,u}(t)} \quad \text{(Eq. 16a)}$$

Both in the case of serum and urine, the reactions creating the end metabolites, $m_{8:10}$ and $m_{6:7}$ are assumed to be in a steady state condition. If the measurements of these end metabolites are made using the second assay with the CYP24A1 hydroxylase enzyme, the same mathematical expressions are used. However, the reactions creating the end metabolites, $m_{8:10}$ and $m_{6:7}$ would be driven to their end metabolites eliminating any intermediate metabolites by addition of the CYP24A1 hydroxylase enzyme. Again, the initial level of $25(OH)D_3$ in the serum and urine must be measured and subtracted from the final $m_{6:7}$ levels to get an accurate measurement of actual $m_{6:7}$ in the plasma or urine.

3.3. The m_0 Utilization Percent

The m_0 utilization percent at any one point in time (t) is defined as the ratio of the nmols of $m_{8:10,i+e}$ (t) divide divided by the nmoles of $m_{8:10,i+e}$ (t) plus $m_{6:7,i+e}$ (t) times 100%. Using the same derivations used in 4. above:

$$Ut\%m_{0,i+e}(t) = \frac{M_{8:10,u}(t)}{M_{*:10}(t) + M_{6:7}(t)} \times 100\% \quad \text{(Eq. 17a)}$$

The 24 h m_0 utilization percent is defined as the ratio of the change in the nmols of $m_{8:10}(t_1,t_0)$ in the intracellular and extracellular compartments plus the accumulation of $m_{8:10}(t_0,t_1)$ in the urine and stool over 24 h divided by the sum of the total $m_{8:10}$ (t_0,t_1) metabolites described above plus the change in the nmols of $m_{6:7}(t_1,t_0)$ in the intracellular and extracellular compartments plus the accumulation of $m_{6:7}(t_0,t_1)$ nmols in the urine and stool over 24 h.

$$\int_{t_0}^{t_1} U'\, t\%m_0\, dt = \frac{\int_{t_0}^{t_1} S_{0,1}\ (t)dt}{\int_{t_0}^{t_1} S_{0,1}\ (t)dt + \int_{t_0}^{t_1} S_{0,2:3}\ (t)dt} \times 100\% \qquad \text{(Eq. 18a)}$$

The integral in the numerator position of Eq.18a represents the sum of the end metabolites of m_1 ($1,25(OH)_2D_{3)}$. For males it is determined by Eq.9a and for females, Eq.10a. The denominator is made up of the integral in the numerator position plus the integral of the end metabolites of $25(OH)D_3$ that are diverted away from the synthesis of $1,25(OH)_2D_3$ and are in fact wasted. This second term in the denominator is determined by Eq. 11a for males or Eq. 12a for females. This integral ratio is then multiplied by 100% to determine the percent utilization of the precursor, $25(OH)D_3$ that is used to make active vitamin D, $1,25(OH)_2D_3$ at any given point in time.

3.4. Percent Increase or Decrease of the above Parameters over Time

Percent increase or decrease of the parameters above including estimates of synthesis of active vitamin D over 24 h, active vitamin D demand ratios, $25(OH)D_3$ percent utilization, and biomarkers for total active vitamin D synthesis at any time t, over the time interval t_{n+1} and t_n can be determined by taking the ratio of a parameter at time t_{n+1} divided by the same parameter at time t_n, minus 1, and then times 100%. For the demand ratio of m_1 as an example:

$$\{[\underline{Drm_{1,i+e}(t_{n+1})} \div (Drm_{1,i+e}(t_n)] - 1\} \times 100\% \qquad \text{(Eq. 19a)}$$

If the same technology to determine the above parameters is used by different labs, and if the measurements which are made at different labs have consistent measurement techniques, variations in parameter values between sequential runs and between labs should be controlled and not significant.

References

1. Chan, T.H. The Nutrition Source. Vitamin D, Harvard School of Public Health. Vitamin D | The Nutrition Source | Harvard T.H. Chan School of Public Health. Available online: https://www.hsph.harvard.edu/nutritionsource/vitamin-d (accessed on 14 December 2022).
2. Panagiotou, G.; Tee, S.A.; Ihsan, Y.; Athar, W.; Marchitelli, G.; Kelly, D.; Boot, C.S.; Stock, N.; Macfarlane, J.; Martineau, A.R.; et al. Low serum 25-hydroxyvitamin D (25[OH]D) levels in patients hospitalised with COVID-19 are associated with greater disease severity: Results of a local audit of practice. *Clin. Endocrinol.* **2020**, *93*, 508–511. [CrossRef] [PubMed]
3. Carpagnano, G.E.; Di Lecce, V.; Quaranta, V.N.; Zito, A.; Buonamico, E.; Capozza, E.; Palumbo, A.; Di Gioia, G.; Valerio, V.N.; Resta, O. Vitamin D deficiency as a predictor of poor prognosis in patients with acute respiratory failure due to COVID-19. *J. Endocrinol. Investig.* **2021**, *44*, 765–771. [CrossRef]
4. Goddek, S. Vitamin D3 and K2 and their potential contribution to reducing the COVID-19 mortality rate. *Int. J. Infect. Dis.* **2020**, *99*, 286–290.
5. Castillo, M.E.; Costa, L.M.E.; Barrios, J.M.V.; Diaz, J.F.A.; Miranda, J.L.; Bouillon, R.; Gomez, J.M.Q. Effect of calcifediol treatment and best available therapy verses best available therapy on intensive care unit admission and morality among patients hospitalized for COVID-19: A pilot randomized clinical study. *J. Steroid Biochem. Mol. Biol.* **2020**, *203*, 105715. [CrossRef]
6. Ye, K.; Tang, F.; Liao, X.; Shaw, B.A.; Deng, M.; Huang, G.; Qin, Z.; Peng, X.; Xiao, H.; Chen, C.; et al. Does Serum Vitamin D Level Affect COVID-19 Infection and Its Severity?-A Case-Control Study. *J. Am. Coll. Nutr.* **2020**, *40*, 724–731. [CrossRef] [PubMed]
7. Meltzer, D.O.; Best, T.J.; Zhang, H.; Vokes, T.; Arora, V.; Solway, J. Association of Vitamin D Status and Other Clinical Characteristics With COVID-19 Test Results. *JAMA Netw. Open* **2020**, *3*, e2019722. [CrossRef] [PubMed]
8. Grant, W.B.; Lahore, H.; McDonnell, S.L.; Baggerly, C.A.; French, C.B.; Aliano, J.L.; Bhattoa, H.P. Evidence that Vitamin D Supplementation Could Reduce Risk of Influenza and COVID-19 Infections and Deaths. *Nutrients* **2020**, *12*, 988. [CrossRef]
9. Lanham-New, S.A.; Webb, A.R.; Cashman, K.D.; Buttriss, J.L.; Fallowfield, J.L.; Masud, T.; Hewison, M.; Mathers, J.C.; Kiely, M.; Welch, A.A.; et al. Vitamin D and SARS-CoV-2 virus/COVID-19 disease. *BMJ Nutr. Prev. Health* **2020**, *3*, 106–110. [CrossRef]

10. Adams, J.S.; Hewison, M. Unexpected actions of vitamin D: New perspectives on the regulation of innate and adaptive immunity. *Nat. Clin. Pract. Endocrinol. Metab.* **2008**, *4*, 80–90. [CrossRef]
11. Hewison, M. Vitamin D and the intracrinology of innate immunity. *Mol. Cell. Endocrinol.* **2010**, *321*, 103–111. [CrossRef]
12. Charoenngam, N.; Holick, M.F. Immunologic Effects of Vitamin D on Human Health and Disease. *Nutrients* **2020**, *12*, 2097. [CrossRef] [PubMed]
13. InformedHealth.org. [Internet. Cologne, Germany: Institute for Quality and Efficiency]. 2020. Available online: https://www.ncbi.nlm.nih.gov/books/NBK279395/ (accessed on 30 November 2021).
14. Biegalski, H.K. Vitamin D deficiency and co-morbidities in COVID-19 patients—A fatal relationship? *Nfs J.* **2020**, *20*, 10–21.
15. Lindo, A.; Lushington, G.H.; Abello, J.; Melgarejo, T. Clinical Relevance of Cathelicidin in Infectious Disease. *J. Clin. Cell Immunol.* **2013**, *S13*, 1–11.
16. Youssef, D.A.; Miller, C.W.; El-Abbassi, A.M.; Cutchins, D.C.; Cutchins, C.; Grant, W.B.; Peiris, A.N. Antimicrobial implications of vitamin D. *Derm.-Endocrinol.* **2011**, *3*, 220–229. [CrossRef]
17. Sassi, F.; Tamone, C.; D'Amelio, P. Vitamin D: Nutrient, Hormone, and Immunomodulator. *Nutrients* **2018**, *10*, 1656. [CrossRef]
18. Calton, E.K.; Keane, K.N.; Newsholme, P.; Soares, M.J. The Impact of Vitamin D Levels on Inflammatory Status: A Systematic Review of Immune Cell Studies. *PLoS ONE* **2015**, *10*, e0141770. [CrossRef] [PubMed]
19. Speddings, S.; Vanlint, S.; Morris, H.; Scraggs, R. Does Vitamin D Sufficiency Equate to a Single Serum 25-Hydroxy Vitamin D level or Are Different Levels Required for Non-Skeletal Diseases? *Nutrients* **2013**, *5*, 5127–5139.
20. Schoenmakers, I.; Jones, K.S. Metabolism and Determinants of Metabolic Fate of Vitamin D. In *Vitamin D Vol. 1, Biochemistry, Physiology, and Diagnostics*, 4th ed.; Feldman, D., Pike, J.W., Bouillon, R., Giovannucci, E., Goltzman, D., Hewison, M., Eds.; Academic Press: Cambridge, MA, USA; Elsevier Inc: Amsterdam, The Netherlands, 2018; p. 642.
21. Need, A.G.; O'Loughlin, P.D.; A Morris, H.; Coates, P.S.; Horowitz, M.; Nordin, B.C. Vitamin D Metabolites and Calcium Absorption in Severe Vitamin D Deficiency. *J. Bone Miner. Res.* **2008**, *23*, 1859–1863. [CrossRef]
22. Jones, G.; Prosser, D.; Kaufmann, M. Thematic Review Series: Fat-Soluble Vitamins: Vitamin D, Cytochrome P450-mediated metabolism of vitamin D. *J. Lipid Res.* **2014**, *55*, 13–31.
23. Tamblyn, J.A.; Jenkinson, C.; Larner, D.P.; Hewison, M.; Kilby, M.D. Serum and urine vitamin D metabolite analysis in early preeclampsia. *Endocr. Connect.* **2018**, *7*, 199–210. [CrossRef]
24. Fairbrother, B.; Shippee, R.L.; Kramer, T.; Askew, W.; Mays, M.; Popp, K.; Kramer, M.; Hoyt, R.; Tulley, R.; Rood, J.; et al. *Nutritional and Immunological Assessment of Soldiers During the Special Forces Assessment and Selection Course*; Technical Report T95-22; U.S. Army Research Institute of Environmental Medicine: Natick, MA, USA, 1995. Available online: https://apps.dtic.mil/dtic/tr/fulltext/u2/a299556.pdf (accessed on 19 January 2019).
25. Jones, K.S.; Redmond, J.; Fulford, A.J.; Jarjou, L.; Zhou, B.; Prentice, A.; Schoenmakers, I. Diurnal rhythms of vitamin D binding protein and total and free vitamin D metabolites. *J. Steroid Biochem. Mol. Biol.* **2017**, *172*, 130–135. [CrossRef]
26. French, C.B.; McDonnell, S.L.; Vieth, R. 25-Hydroxyvitamin D variability within-person due to diurnal rhythm and illness: A case report. *J. Med. Case Rep.* **2019**, *13*, 1–5. [CrossRef] [PubMed]
27. Jolliffe, D.A.; Walton, R.T.; Griffin, C.J.; Martinean, A.R. Single nucleotide polymorphism in the vitamin D pathway associating with circulating concentrations of vitamin D metabolites and non-skeletal outcomes-Review of genetic association studies. *J. Steroid. Biochem. Mol. Biol.* **2016**, *164*, 18–29. [CrossRef] [PubMed]
28. St-Arnaud, R.; Jones, G. CYP24A1: Structure, Function, and Physiological Role. In *Vitamin D Vol. 1, Biochemistry, Physiology, and Diagnostics*, 4th ed.; Feldman, D., Pike, J.W., Bouillon, R., Giovannucci, E., Goltzman, D., Hewison, M., Eds.; Academic Press: Cambridge, MA, USA; Elsevier Inc.: Amsterdam, The Netherlands, 2018; pp. 82–84.
29. Fagerberg, L.; Hallström, B.M.; Oksvold, P.; Kampf, C.; Djureinovic, D.; Odeberg, J.; Habuka, M.; Tahmasebpoor, S.; Danielsson, A.; Edlund, K.; et al. Analysis of the Human Tissue-Specific Expression by Genome-wide Integration of Transcriptions and Antibody based Proteomics. *Mol. Cell. Proteom.* **2014**, *13*, 397–406.
30. PKM-Array Suite WIKI. Report Gene Transcript Counts. Available online: https://wiki.arrayserver.com/wiki/index.php?title=Array_Suite_Wiki (accessed on 2 August 2022).
31. CYP27A1 Cytochrome P450 Family 27 Subfamily A Member 1 [Homo Sapiens (Human)] HPA RNA-Seq. Normal Tissues, Bio Project PRJEB 4337, PMID 24309898. Available online: https://www.ncbi.nlm.nih.gov/gene/1593 (accessed on 2 August 2022).
32. CYP2R1 Cytochrome P450 Family 2 Subfamily R Member 1 [Homo Sapiens (Human)]. HPA RNA- Seq. Normal Tissues, Bio Project PRJEB 4337, PMID 24309898. Available online: https://www.ncbi.nlm.nih.gov/gene?Db=gene&Cmd=DetailsSearch&Term=120227 (accessed on 2 August 2022).
33. CYP3A4 Cytochrome P450 Family 3 Subfamily A Member 4 [Homo Sapiens (Human)]. Available online: https://www.ncbi.nlm.nih.gov/gene/1576 (accessed on 2 August 2022).
34. CYP27B1 Cytochrome P450 Family 27 Subfamily B Member 1 [Homo Sapiens (Human)]. Available online: https://www.ncbi.nlm.nih.gov/gene?Db=gene&Cmd=DetailsSearch&Term=1594 (accessed on 2 August 2022).
35. CYP24A1 Cytochrome P450 Family 24 Subfamily A Member 1 [Homo Sapiens (Human)]. Available online: https://www.ncbi.nlm.nih.gov/gene?Db=gene&Cmd=DetailsSearch&Term=1591 (accessed on 2 August 2022).
36. Ciprini, C.; Pepe, J.; Piemonte, S.; Colangelo, L.; Cilli, M.; Minisola, S. Review Article: Vitamin D and Its Relationship with Obesity and Muscle. *Int. J. Endocrinol.* **2014**, *2014*, 841248.
37. Ceglia, L. Vitamin D and its role in skeletal muscle. *Curr. Opin. Clin. Nutr. Metab. Care* **2009**, *12*, 628–633.

38. Girgis, C.M.; Clifton-Bligh, R.J.; Mokbel, N.; Cheng, K.; Gunton, J.E. Vitamin D Signaling Regulates Proliferation, Differentiation, and Myotube Size in C2C12 Skeletal Muscle Cells. *Endocrinology* **2014**, *155*, 347–357. [CrossRef]
39. Molner, F.; Sigueiro, R.; Sato, Y.; Araujo, C.; Schuster, I.; Antony, P.; Peluso, J.; Muller, C.; Mourino, A.; Moras, D.; et al. 1α,25(OH)$_2$-3-Epi-Vitamin D$_3$, a Natural Physiological Metabolite of Vitamin D$_3$: Its Synthesis, Biological Activity and Crystal Structure with Its Receptor. *PLoS ONE* **2011**, *6*, e18124. [CrossRef]
40. Schoenmakers, I.; Jones, K.S. Muscle and Adipose Tissue. In *Vitamin D Vol. 1, Biochemistry, Physiology, and Diagnostics*, 4th ed.; Feldman, D., Pike, J.W., Bouillon, R., Giovannucci, E., Goltzman, D., Hewison, M., Eds.; Academic Press: Cambridge, MA, USA; Elsevier Inc.: Amsterdam, The Netherlands, 2018; p. 641.
41. Heaney, R.P.; Horst, R.L.; Cullen, D.M.; Armas, L.A.G. Vitamin D$_3$ distribution and status in the body. *J. Am. Coll. Nutr.* **2009**, *28*, 252–256.
42. Avioli, L.V.; Lee, S.W.; McDonald, J.L.; DeLuca, H.F. Metabolism of Vitamin D$_3$−^{3}H in Human Subjects: Distribution in Blood, Bile, Feces, and Urine. *J. Clin. Investig.* **1967**, *46*, 983–992.
43. Gray, R.W.; Caldas, A.E.; Wilz, D.R.; Lemann Jr, J.; Smith, G.A.; DeLuca, H.F. Metabolism and excretion of ^{3}H−1,25(OH)$_2$ vitamin D$_3$ in Healthy Adults. *J. Clin. Endocrinol. Metab.* **1978**, *46*, 756–765. [CrossRef] [PubMed]
44. Kumar, S.R.; Hunder, G.G.; Heath, H.I.I.I.; Riggs, B.L. Production, Degradation, and Circulating Levels of 1,25- Dihydroxyvitamin D in Health and in Chronic Glucocorticoid Excess. *J. Clin. Investig.* **1980**, *66*, 664–669.
45. Physiology Figure: Body Fluid Compartments of a 55-Kg Adult Woman. Available online: https://www.physiologyweb.com/figures/figs/body_fluid_compartments_adult_female_jpg_n9MxaD4XkTrQmJaIzfPLxmOjYSmwvURv.html (accessed on 4 August 2022).
46. Physiology Figure: Body Fluid Compartments of a 70-Kg Adult Man. Available online: https://www.physiologyweb.com/figures/physiology_illustration_tPksfgTyDcZ10zEq1Wp1FqLjrBRL8IGL_body_fluid_compartments_of_a_70_kg_adult_man.html (accessed on 4 August 2022).
47. Vitamin D-Dependent Rickets, Genetics Home Reference. U.S. National Library of Medicine, NIH. Available online: https://ghr.nlm.nih.gov/condition/vitamin-d-dependent-rickets#genes (accessed on 4 August 2022).
48. Pasquali, M.; Tartaglione, L.; Rotondi, S.; Muci, M.L.; Mandanici, G.; Farcomeni, A.; Marangella, M.; Mazzaferro, S. Calcitriol/calcifediol ratio: Indicator of vitamin D hydroxylation efficiency? *BBA Clin.* **2015**, *3*, 251–256.
49. Zelser, S.; Goessler, W.; Herrmann, M. Measurement of vitamin D metabolites by mass spectrometry, and analytical challenge. *J. Lab. Precis. Med.* **2018**, *3*, 1–14.
50. Müller, M.J.; Volmer, D.A. Mass Spectrometric Profiling of Vitamin D Metabolites beyond 25-Hydroxyvitamin D. *Clin. Chem.* **2015**, *61*, 1033–1048. [CrossRef]
51. Abu Kassim, N.S.; Shaw, P.N.; Hewavitharana, A.K. Simultaneous determination of 12 vitamin D compounds in human serum using online sample preparation and liquid chromatography-tandem mass spectrometry. *J. Chromatogr. A* **2018**, *1533*, 57–65. [CrossRef]
52. Sofiah, N.; Kassim, A. Development of an Assay for Vitamin D in Biological Samples. Ph.D. Thesis, University of Queensland, Brisbane, Australia, 2017. Available online: https://espace.library.uq.edu.au/view/UQ:728352 (accessed on 15 May 2020).
53. Calcitroic Acid & Calcioic Acid. Toronto Research Chemicals. 20 Martin Ross Ave, North York, ON M3J 2K8, Canada 1-416-665-9696, (USA and Canada 1-800-727-9240). Available online: https://www.trc-canada.com/products-listing/ (accessed on 30 October 2020).
54. CYP24A1 (Human) Recombinant Protein, Biocompare.Com. Available online: https://biocompare.com/Search-Biomolecules/?search=CYP24A1 (accessed on 17 July 2020).
55. Sakaki, T.; Sawada, N.; Nonaka, Y.; Ohyama, Y.; Inouye, K. Metabolic studies using recombinant Escherichia coli cells producing rat mitochondrial CYP24−CYP24 can convert 1α,25-dihydroxyvitamin D$_3$ to calcitroic acid. *Eur. J. Biochem.* **1999**, *262*, 43–48.
56. McGonagle, D.; Sharif, K.; O'Regan, A.; Bridgewood, C. The Role of Cytokines including Interleukin-6 in COVID-19 induced Pneumonia and Macrophage Syndrome-Like Disease. *Autoimmun. Rev.* **2020**, *19*, 102537.
57. Kaufman, H.W.; Niles, J.K.; Kroll, M.H.; Bi, C.; Holick, M.F. SARS-CoV-2 positivity rates associated with circulating 25-hydroxyvitamin D levels. *PLoS ONE* **2020**, *15*, e0239252. [CrossRef]